

How to Train Your Filter: Should You Learn, Stack or Adapt?

Diandre Miguel Sabale

 Northeastern University

Boston, MA, USA

sabale.d@northeastern.edu

Wolfgang Gatterbauer

 Northeastern University

Boston, MA, USA

w.gatterbauer@northeastern.edu

Prashant Pandey

 Northeastern University

Boston, MA, USA

p.pandey@northeastern.edu

Abstract

Filters are ubiquitous in computer science, enabling space-efficient approximate membership testing. Since Bloom filters were introduced in 1970, decades of work have improved their space efficiency and performance. Recently, three new paradigms have emerged that offer orders-of-magnitude improvements in false positive rates (FPRs) by leveraging additional information beyond the input set: (1) *learned filters* train a model to separate members from non-members, (2) *stacked filters* use negative workload samples to build cascading layers, and (3) *adaptive filters* update internal representation in response to false positive feedback. Yet each paradigm targets specific use cases, introduces complex configuration tuning, and has been evaluated only in isolation. This results in unclear trade-offs and a significant gap in understanding how these approaches compare and when each is most appropriate.

This paper presents the first comprehensive comparative evaluation of learned, stacked, and adaptive filters across real-world datasets and diverse query workloads. Our results reveal critical trade-offs: (1) *Learned filters* achieve up to $10^2 \times$ lower FPRs when query distributions match training data, but exhibit high variance and lack robustness under skewed or dynamic workloads. Critically, learned filters' inference overhead leads to up to $10^4 \times$ slower query latencies than stacked and adaptive filters. (2) *Stacked filters* reliably achieve up to $10^3 \times$ lower FPRs on skewed workloads but require prior knowledge of the workload. (3) *Adaptive filters* are robust across all settings, achieving up to $10^3 \times$ lower FPRs under adversarial queries without workload assumptions. Based on our analysis, *learned filters* suit stable workloads where input features enable effective model training and space constraints are paramount, *stacked filters* excel when query distributions are known in advance and relatively static, and *adaptive filters* are the most general option, providing robust guarantees backed by theoretical bounds even for dynamic and adversarial environments.

1 Introduction

A *filter* (such as Bloom [5], quotient [4, 35], cuckoo [20], XOR [23], or ribbon [16]) provides an approximate representation of a set and saves space by trading off accuracy through one-sided errors (no false negatives) in membership queries. These errors are bounded by a configurable false positive rate (FPR).

Filters are ubiquitous across computer science and have long served as fundamental building blocks in applications where memory constraints are important and one-sided errors are acceptable [8, 10, 11, 15, 17, 31, 33, 34, 36, 38].

Since Bloom's seminal work in 1970 [5], there have been decades of progress in filter design. Dynamic filters such as quotient filters [4, 35] and cuckoo filters [20] improved upon Bloom filters by supporting deletions and achieving better cache performance. More recently, static filters such as XOR filters [23] and ribbon filters [16]

have pushed space efficiency closer to the information-theoretic optimum.¹ With over a thousand papers on filter data structures published in the last two decades,² these advancements have collectively improved both space utilization and query performance, making filters increasingly efficient for their traditional use cases.

Modern paradigms in filter design. Recently, three new paradigms in filter design have emerged that offer orders-of-magnitude improvements in false positive rates by leveraging additional information beyond the input set alone. Figure 1 summarizes these approaches, each optimized for different assumptions about available data, workload knowledge, and query feedback.

- (1) **Learned filters** [25, 28] exploit correlations between element features and dataset distributions by training a model to distinguish keys that are not part of the set from those that are. Queries first consult the trained model and only proceed to a backup filter if the model predicts a negative result. State-of-the-art implementations such as Fast Partitioned Learned Bloom Filters (PLBF) [44, 49], ADA-BF [12], and Sandwiched Learned Bloom Filters [28] can achieve up to $10 \times$ lower false positive rates compared to Bloom filters at equivalent space.
- (2) **Stacked filters** [14] leverage workload knowledge from query samples to build cascading layers of filters that suppress false positives on frequently queried negatives. By storing these frequent positives across layers, they often outperform learned filters on skewed workloads.
- (3) **Adaptive filters** [3, 29, 50] adjust their internal structure in response to feedback from false positive results. By maintaining a disk-resident *reverse map* that recalls the original key causing a false positive, adaptive filters can extend their structure to avoid repeating the same mistake during future queries. This provides a much stronger guarantee than traditional filters: bounded false positive rates for *any* arbitrary sequence of queries, rather than only for queries drawn uniformly at random. The state-of-the-art adaptive filter, ADAPTIVEQF [50], achieves up to $100 \times$ lower false positive rates compared to traditional filters.

Why it is challenging to navigate the design space. These paradigms introduce several new design knobs (model choice, training strategy, layer layouts, and feedback policies) that require careful tuning to achieve desired performance. Furthermore, all three paradigms have been defined and evaluated primarily within their respective settings, without a unified evaluation framework to draw meaningful conclusions about how they compare to one another.

This creates a significant gap in our understanding of modern filter paradigms. Systems designers face a daunting landscape: several tuning knobs, diverse application requirements, and disparate performance characteristics. At the same time, there is a lack of clear guidance on how to navigate these choices. Existing learned filter

¹The lower bound on space usage for a dynamic filter is $n \log(1/\epsilon) + \Omega(n)$ bits [35].

²We searched for Bloom filters on DBLP and got 1,130 results.

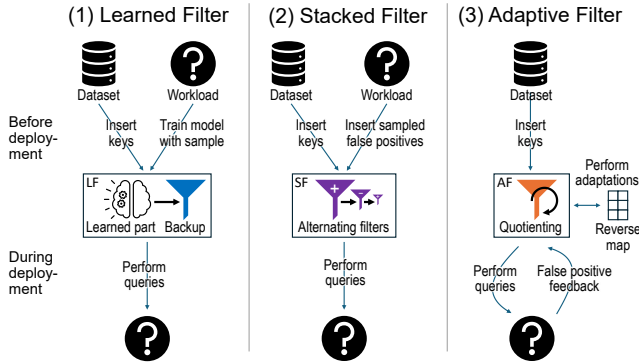


Figure 1: Before deployment, learned filters train on dataset features and stacked filters train on sampled negative queries. During deployment, adaptive filters update on false positive feedback.

evaluations focus only on stable, predictable workloads and often compare primarily against Bloom filters, despite stronger modern baselines (e.g., cuckoo/quotient/xor filters). Critical metrics such as the computational overhead of model inference and the impact of model sizing have been largely overlooked, potentially overstating the practical benefits of learned approaches.

Our contribution. In this paper, we aim to fill this information gap through a comprehensive evaluation and comparison of learned, stacked, and adaptive filters.³ Our contributions include:

- **Unified evaluation:** We provide the first comprehensive comparison of learned, stacked, and adaptive filters under a unified evaluation framework, featuring direct performance comparisons across diverse workloads and datasets.
- **Robustness analysis:** We evaluate filter performance under adversarial attacks, dynamic workload distributions, and repeated query patterns: conditions that stress-test the assumptions underlying each filter paradigm.
- **Computational overhead analysis:** We measure and report the full computational costs of each filter type, including model training and inference overhead for learned filters, constructing cascading layers for stacked filters, and adapting and reverse map maintenance for adaptive filters.
- **Configuration sensitivity study:** We analyze how key learned filter configuration parameters, such as the choice of model, model size allocation, and training set size, affect their overall performance.
- **Use case recommendations:** We provide evidence-based guidance for selecting appropriate filter types based on application requirements, including query distribution stability, computational constraints, and robustness needs.

Key Findings. Learned filters demonstrate improved accuracy compared to adaptive and stacked filters under specific conditions. When query distributions closely match training distributions, learned filters achieve considerably better FPRs compared to the other filters (close to $10^2 \times$ better (Fig. 8)). However, learned filters can suffer from high variance in observed false positive rates and lack robustness

³We study approximate membership/equality filters that answer ‘is key x in set S ?’ with no false negatives and tunable FPR. We do not study range filters, probabilistic predicates beyond membership, or learned index structures; our focus is the design space of learned, stacked (workload-trained), and adaptive (feedback-driven) membership filters.

guarantees against adversarial attacks (Fig. 11) and dynamic workloads (Fig. 12), even when model rebuilding is allowed. In particular, for skewed workloads, learned filter false positive rates can even fluctuate from 1% to over 40% when *increasing* the space budget (Fig. 10).

Critically, our analysis demonstrates that the computational cost of querying learned models frequently exceeds that of traditional filter operations (up to $10^4 \times$ slower (Fig. 14)), challenging the practical value proposition of learned filters in many applications. This finding is particularly significant given that existing evaluations have largely overlooked model querying costs, potentially overstating the benefits of learned approaches.

Stacked filters, by contrast, often achieve lower false positive rates across diverse datasets and query patterns for equivalent space allocations because of their use of workload knowledge. For example, on queries following a Zipfian distribution, they can reach false positive rate improvements of up to $10^5 \times$ (Fig. 10) compared to some variants of learned filters.

Adaptive filters provide robust theoretical guarantees and demonstrate low false positive rates across different datasets and query patterns. On workloads where the query distribution changes adversarially, the adaptive filter’s false positive rates can be up to $10^3 \times$ (Fig. 11) lower than other filters. Adaptive filters also offer the fastest query and construction performance, beating stacked filters (the next best filter) by up to 3×. Adaptive filters demonstrate dependable performance regardless of dataset characteristics, consistently decreasing the false positive rate as more space is allocated (Fig. 8, Fig. 9, Fig. 10).

We also demonstrate new findings regarding learned filter configurations. We show that the proportion of negative keys in the training set has little effect on the final learned filter performance, with median false positive rates having ranges close to 0 across different proportions (Fig. 7). We also find that assigning too much relative space to the trained model within a learned filter’s space budget has adverse effects on performance, with the filters exhibiting false positive rates well over 10% when the majority of the space is dedicated to the model (Fig. 6).

Through validation of theoretical results and comprehensive experimental analysis, this work establishes specific application requirements to guide a choice between learned, stacked and adaptive filters. With their high space efficiency on predictable workloads, learned filters are suitable for stable workloads where the features of input keys can be meaningfully used to improve model decisions and inference cost overheads are not critical. Meanwhile, the robustness and higher-speed operations of adaptive and stacked filters make them useful for general settings, with benefits in particular for dynamic, security-sensitive, or high-workload applications. Adaptive filters specifically are not constrained by knowledge about the query workload and are the most generalizable filter.

2 Learned filters

A *learned filter* combines a machine learning model with a traditional filter (usually a Bloom filter [12, 44]) to improve the space-accuracy trade-off for approximate membership testing. The learned filter operates in two stages during deployment:

- (1) **Model prediction.** When a query arrives, the filter takes extracted features from the key and passes them to a trained machine learning model. The model outputs a confidence score

$s \in [0, 1]$ indicating the likelihood that the key belongs to the positive set.

(2) **Threshold decision.** If the score exceeds a predetermined threshold t (meaning $s \geq t$), the filter immediately returns "positive". If the score is below the threshold ($s < t$), the query is passed to a backup traditional filter for the final decision.

Training process. The model is trained on a dataset containing both positive examples (keys that should return "yes") and negative examples (keys that should return "no"). For a given key, features suitable as ML model input can either be extracted from the key or given as separate input. The training process learns correlations between features of keys and their membership status. For example, in malicious URL detection, features might include URL length, domain characteristics, and character patterns [40]. In malware detection, features could include file size, system versions, and other important metadata [2].

Key insight. The learned model acts as a "smart pre-filter" that identifies likely positives based on learned patterns, allowing the backup filter to be smaller since it only handles the remaining uncertain cases. When the model correctly identifies positives, it saves space because those keys do not need to be stored in the backup filter. The backup filter also ensures the overall structure maintains the guarantee of a 0% false negative rate even if the model makes a mistake.

Critical dependency. The improved effectiveness of learned filters strongly depends on the quality of the underlying machine learning model and the assumption that query patterns will match training patterns. When these assumptions break down (as often happens in practice) the filter's performance can degrade significantly, sometimes performing worse than traditional approaches.

Note that for a learned filter, false positives from the ML model due to high scores become false positives in the overall output. Thus, the FPR of the learned filter is floored by the FPR of its ML model. Concretely, if the model has a FPR f_m and its backup filter structure has a FPR f_b , then the overall FPR of a learned filter is $f_m + (1 - f_m)(f_b)$ [28]. Due to their dependence on model quality, learned filters tend to be used in cases where there is a direct correlation between the features of an element and the likelihood of its presence in a set.

Mitzenmacher [28] also introduces the *sandwiched learned Bloom filter*. In a sandwiched learned Bloom filter, an additional filter is employed before the trained model to process queries and immediately return true negatives. This additional step reduces the number of potential false positives that the rest of the learned filter processes.

2.1 Theoretical guarantees

Behavior of learned models. Mitzenmacher [28] used a Chernoff bound to prove a theorem suggesting that the empirical FPR of a learned filter on a test set will be close to the FPR on future queries *assuming that the test set has the same distribution as future queries*. We will experimentally demonstrate that when this assumption does not hold, learned filters cannot strongly guarantee their performance, resulting in substantial deviations in empirical FPRs.

Size of learned models. Analysis from [28] also describes how the size of the learned model relates to its expected effectiveness compared to standard Bloom filters.

THEOREM 1. [28] Consider a learned Bloom filter with n keys, b bits per key used by the backup filter, and slot fill rate α . For its learned

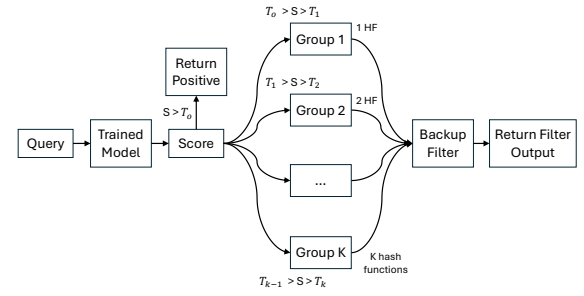


Figure 2: ADA-BF structure. Keys are assigned a number of hash functions depending on the model's predicted likelihood of them being a positive element. The bits corresponding to all their hashes are used for insertions and queries.

function using ζ bits, let f_m be the false positive probability, and f_n the false negative probability. The learned filter is expected to outperform a Bloom filter using the same space budget when

$$\zeta/n \leq \log_\alpha(f_m + (1 - f_m)\alpha^b/f_n) - b$$

A bound can be applied to the number of bits per key the learned function should be allotted to outperform standard filters. Intuitively, as the amount of space dedicated to the learned function increases, it has a reduced benefit from the backup filters, eventually worsening its performance. We will experimentally demonstrate how changing the proportion of space dedicated to the learned function influences the performance of the overall learned filter.

2.2 Ada-BF

ADA-BF expands on the basic learned Bloom filter by adapting insertions and queries into the backup filter according to the internal model's predictions [12]. The structure is described in Fig. 2.

First, it splits queries into k groups. Group assignments depend on the model's score for the input key, which describes the likelihood that the key is a positive element. The score thresholds to divide the groups are optimized according to a constant c such that each group is expected to contain c times more non-keys than the next group. Within each group, keys are assigned a certain number of hash functions. Groups with more keys are assigned increasingly larger numbers of hash functions, up to k .

During an insertion, a key is assigned a group according to its model score, then all the bits in the backup filter corresponding to its hashes are set. A query checks those same bits if the model predicts that the query is a negative key. Intuitively, to avoid false positives, groups with more keys should check more bits in the backup filter to reduce the chances of a hash collision.

2.3 PLBF

The Partitioned Learned Bloom Filter (PLBF) expands on the basic learned Bloom filter by assigning keys to different backup filters depending on their model scores. The structure is described in Fig. 3.

Similarly to ADA-BF, the PLBF divides keys into k groups based on their assigned scores from an internal ML model. Each group has its own backup filter, which is optimized for the space budget and targeted overall FPR. In our experiments, we use the FAST PLBF

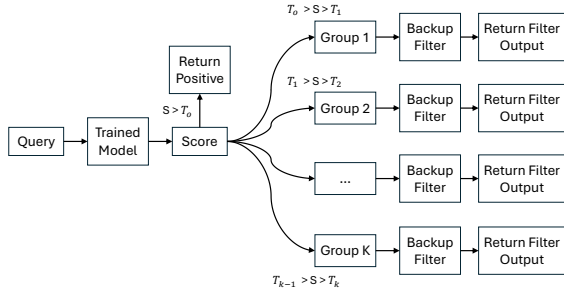


Figure 3: Partitioned learned Bloom filter (PLBF) Structure. Keys are assigned to different backup filters depending on the score assigned to them by a model.

implementation [44], which uses a dynamic programming approach to efficiently construct the filter by splitting the score space into N segments which are assigned to k groups.

When a key is inserted, it is assigned a group according to its model score, then inserted into that group's backup filter. On a query, if the model predicts the key may be a negative, the filter belonging to the key's group is checked. The intuition is that keys that are likely to be negative should use larger backup filters to reduce their false positives; meanwhile, keys with higher scores use smaller backup filters, since false positives on keys which were likely true positives have less impact on the overall FPR.

3 Stacked filters

Stacked filters [14] exploit knowledge of the query workload to reduce false positive rates. By storing frequently queried negative keys across cascading filter layers, the structure adapts to the distribution of the query set.

A stacked filter consists of alternating layers that store either positive or negative keys. Construction proceeds as follows: the first layer stores all positive keys (keys that are part of the set). From a sample of negative queries, any false positives of the first layer are stored in the second layer. Any positive values that collide with the second layer are then stored in the third layer, and so on. This cascading process continues until the space budget is exhausted or the target false positive rate is achieved.

Queries traverse the layers sequentially. At each positive layer, a negative response confirms the element is not in the set. At each negative layer, a negative response indicates the element is likely in the set. The query continues through successive layers until a definitive answer is reached or the final layer makes the decision. Figure 4 illustrates this process on a three-layer stacked filter.

The key insight is that frequent negative queries that would cause false positives in a standard filter are explicitly stored in the stacked filter's negative layers, eliminating these errors. For infrequent negatives, the cascading structure provides protection: an element must pass membership checks across multiple alternating layers, making false positives exponentially unlikely.

Stacked filter construction requires a sample of the query workload to estimate the distribution of negative queries. Given this sample and a space budget, the stacked filter solves an optimization

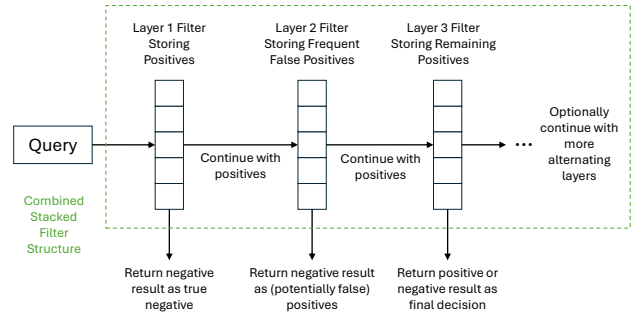


Figure 4: Stacked filter structure. Queries undergo membership queries across layers of filters alternately storing positive and negative queries.

problem to determine the false positive rate for each layer that minimizes the overall false positive rate. The structure is flexible, each layer can use any underlying filter type, including Bloom, quotient, or cuckoo filters.

The expected false positive rate combines two components: the probability that frequent negatives escape the negative layers, and the probability that infrequent negatives pass through all layers. Space usage is the sum of filter sizes across all layers, dominated by the first layer which must store all positive values.

The stacked filter also supports incremental construction through a variant called the adaptive stacked filter [14], which adjusts to the query workload online, provided the query distribution remains relatively stable. This variant initializes with a single layer containing all positive elements. As queries arrive, detected false positives are inserted into a second (negative) layer. Once this layer reaches a target load factor, the filter rescans the positive values to construct a third layer, and subsequent layers are built similarly as needed.

Though adaptive, the adaptive stacked filter lacks theoretical guarantees and empirical performance compared to the ADAPTIVEQF. First, adapting to a false positive requires substantially more space: the stacked filter must store the entire false positive key in a new layer, whereas the ADAPTIVEQF only extends the colliding fingerprint. Second, the ADAPTIVEQF provides stronger theoretical guarantees on false positive rates than the adaptive stacked filter lacks. Third, query performance differs substantially: stacked filters probe multiple layers, incurring multiple cache misses, while the ADAPTIVEQF guarantees single cache-line access for both positive and negative queries, yielding significantly better empirical performance.

Similarity to cascade filters. Stacked filters [14] share conceptual similarities with cascading filters [43], which were introduced in 2014 for representing de Bruijn graphs in genomics. In this application, the filter represents the set of k -mers (length- k sequences) forming nodes in the graph, where edges connect nodes sharing a $(k-1)$ -length overlap. Rather than storing edges explicitly, the filter is queried for all possible extensions of a node, typically bounded by the alphabet size (four nucleotides in genomics). Since graph traversal defines the query set in advance, cascading filters construct successive layers of exponentially decreasing size, each storing false positives from the previous layer, ultimately achieving an exact representation.

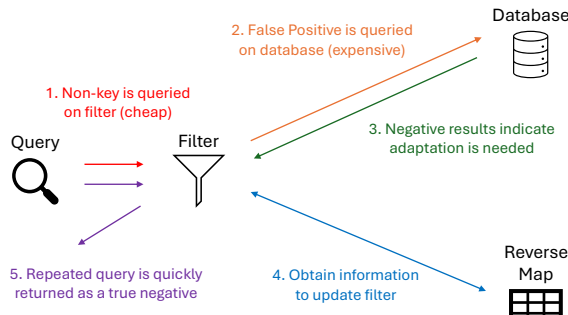


Figure 5: Adaptive filters update their representation upon detecting a false positive to avoid committing the same false positive again. To adapt they employ an on-disk reverse map to access the original key corresponding to the colliding fingerprint. This reverse map is only accessed upon false positives.

4 Adaptive filters

An adaptive filter returns TRUE with probability at most ϵ for every negative query, regardless of answers to previous queries. These were defined by Bender et al. [3, 30], who outlined the filter’s bounds on the number of false positives (even with a skewed or adversarial query distribution) then presented the broom filter which meets their definition. For a database using an adaptive filter, any sequence of $|Q_N|$ negative queries results in $O(\epsilon|Q_N|)$ false positives with high probability. This gives a strong guarantee on the number of (expensive) negative accesses that the database will need to make to disk.

Adaptive filters require two features to support adaptivity. Firstly, they need *feedback* about their false positives. For example, if an adaptive filter is used by an application to avoid database lookups for nonexistent items, then the application can inform the filter that a query for an item x was a false positive if the subsequent database query returned that x is not present. Secondly, adaptive filters also need a *reverse map* to store information to support adaptation. Bender et al. [3] showed that the reverse map is necessary and must be large enough to store the entire set: the total size of an adaptive filter on a set S essentially must be large enough to store S [3]. An example is provided in Figure 5.

The trick is to break the filter into two parts: a small in-memory component accessed on every query and a large reverse map accessed only during adaptations (and hence can reside in slower storage). All proposed adaptive filters use this structure. In some applications, like when the filter is in front of a database, the database may also serve as the reverse map, so that the total storage requirements of the system remain essentially unchanged [50].

Later, Mitzenmacher et al. [29] proposed adaptive cuckoo filters and Lee et al. [26] proposed telescoping filters as implementations of adaptive filters to address the skewed query distribution problem. However, these initial implementations suffer from suboptimal performance due to the inefficient design of the reverse map.

Recently, Wen et al. [50] proposed ADAPTIVEQF, a practical implementation of the adaptive filter based on the quotient filter. ADAPTIVEQF is *monotonically adaptive*, i.e., it never forgets a false positive once adapted. The filter can be resized in case it runs out of space during adaptations and offers strong performance guarantees. We

employ the adaptive quotient filter (ADAPTIVEQF) as the representative adaptive filter as it is the state of the art in terms of performance and theoretical guarantees.

4.1 Adaptive quotient filter

The ADAPTIVEQF makes use of *quotienting*. For an element x , after obtaining its hash $h(x)$, the higher-order q bits are used to obtain a quotient $h_0(x)$ and the lower-order r bits form its remainder $h_1(x)$. Together, the quotient and remainder make up a $q+r = p$ -bit fingerprint. The filter is initialized by allotting 2^q slots for remainders, each with an initial size of r bits. During an insertion of a key x , the filter first obtains $h_0(x)$ and $h_1(x)$ from its hash. $h_0(x)$ is then used to assign the slot to store $h_1(x)$. To query a key, the filter checks if any of the stored elements in the slot corresponding to the queried key’s quotient matches its remainder.

A false positive occurs if the p -bit fingerprint (quotient and remainder) of an existing key matches one that is not in the set. After a false positive query, the stored remainder is extended by the next r bits in the hash of the original key. The *reverse map* stores the mappings of fingerprints to their original inserted key. This mapping allows the filter to find the original key corresponding to the collided fingerprint and determine which bits should be used to extend the fingerprint by recreating the complete hash. By ‘over adapting’ and adding r more bits instead of the minimum required (in expectation 2), the adaptive filter ensures that for some specified FPR ϵ , it never makes errors above that threshold [50].

The original paper demonstrates that with its performance guarantees, the ADAPTIVEQF implementation performs empirically better than other adaptive filters and remains competitive with non-adaptive filters while still maintaining its FPR [50]. The main draw of this filter is its monotonic adaptivity guarantees, allowing its FPR to be dependable for arbitrary query distributions.

5 Experimental methodology

In this section, we extensively evaluate the performance of state-of-the-art learned, adaptive, and stacked filters. Our evaluation aims to fill the gaps in our understanding of the performance of these filters as pointed out in Section G.

Furthermore, we perform an investigation into learned filters to better understand the impact of various configuration parameters. We assess the impact of considerations like the ratio of the model and backup filter(s) sizes or the composition of the model’s training set on the structure’s overall false positive rate.

Our evaluation represents the first direct comparative analysis between learned, adaptive, and stacked filtering paradigms, providing evidence-based guidance for filter selection in practical deployments.

Filters evaluated. We evaluate implementations from each modern paradigm (learned, stacked, adaptive). As representatives, we compare the ADA-BF [12], PLBF [49], stacked filters [14], and the ADAPTIVEQF [50]. We exclude the (sandwiched) learned Bloom filter because ADA-BF, PLBF, and stacked filters all demonstrated superior empirical performance under direct comparisons [12, 14, 44, 49]. We use the FAST PLBF implementation instead of PLBF++ because under some conditions the PLBF++ differs in structure from the PLBF [44]. For all the filters, we employ the open source implementations provided by the original authors. The learned filters [12, 44] are

implemented in Python due to the library support for model training [39], the ADAPTIVEQF [50] is implemented in C language, and the stacked filter [14] is implemented in C++.

Implementation language differences. While the choice of language for filter implementation such as Python or C can introduce differences in run time, we choose to employ the learned filter implementations provided by the original authors due to two main reasons. First, we show in Fig. 14 that for learned filters, the cost of model inference is orders of magnitudes larger than the cost of querying backup filters, contributing to a performance difference too large to be attributed solely to language differences. Second, we want to avoid any author bias when implementing them ourselves in a different language. Our goal is to evaluate the open-source implementations provided by the original authors.

FPR calculation. We also define the reported false positive rate (FPR) in terms of the content of the query set. After performing a set of queries Q on a filter, if $Q_{FP} \in Q$ is the multiset of false positives and $Q_N \in Q$ is the multiset of negatives, then the empirical false positive rate is $FPR = \frac{|Q_{FP}|}{|Q_{FP}| + |Q_N|}$.

5.1 Research questions

Our experimental evaluation aims to address the following questions regarding the relative performance of modern filters:

- (1) How do learned, stacked, and adaptive filters compare in FPR and space efficiency under identical workload conditions?
- (2) How do learned, stacked, and adaptive filters perform under real-world query distributions (uniform, Zipfian, adversarial) versus the stable workloads assumed in current evaluations?
- (3) What are the true computational costs, such as construction time, query throughput (including model inference), and retraining overhead, of learned filters compared to stacked and adaptive filters?
- (4) How do learned filter configuration choices (space allocation, model type, training set composition) affect performance, and do empirical results validate existing theoretical bounds?
- (5) How do learned filters perform on general-purpose datasets lacking strong feature-membership correlations, beyond the specialized domains (malware, URL filtering) used in current evaluations?
- (6) How do learned, stacked, and adaptive filters degrade under dynamic workloads with evolving datasets and shifting query patterns, and what maintenance strategies sustain performance over time?

5.2 Evaluation framework

To address these questions, we conduct a comprehensive experimental evaluation across multiple real-world datasets, diverse query distribution patterns, various performance metrics, and alternative learned model configurations. All code is available [online](#).

Machine specification. All experiments are run on a server with an Intel(R) Xeon(R) Gold 5218 CPU @ 2.30GHz using Linux kernel 5.14.0 and 754 GiB RAM.

5.3 Datasets

We use the real-world Malicious URL, Ember, Shalla, and Caida datasets from the papers that proposed these filters [12, 44, 50]. The datasets are described in Table 1. Shalla [24] and Caida [9] are new for learned filter evaluation, while Malicious URL [46] and Ember [2] are new for adaptive filters. Stacked filters were previously tested on a variant of the Shalla dataset [14].

For the Malicious URL dataset [46], we insert URLs labeled as "malicious" into the filter, while all other URLs are treated as negative keys. For the Ember dataset [2], we insert the SHA-256 hashes of malware into the filter.

For the Shalla dataset [24], since the blacklist consists only of malicious URLs, we combine the dataset with the Cisco Umbrella Top 1M Domains [48], treating any URLs that are not present in the Shalla blacklist as negative keys.

The CAIDA dataset [9] consists of a set of anonymized network traces. To convert the dataset into a classification problem, we filtered the dataset for entries that only followed the TCP or UDP protocols, then treated traces following the UDP protocol as positive keys.

Dataset Name	Overall Keys	Positive Keys
URL	162,798	55,681
Ember	800,000	400,000
Shalla	3,905,928	2,926,705
Caida	8,493,974	1,196,194

Table 1: Summary of datasets.

5.4 Filter construction

For all datasets, we start by constructing an ADAPTIVEQF [50]. Recall that the ADAPTIVEQF has two parameters q and r that control the filter's space usage and FPR (Section 4). If n is the number of unique positive key elements to insert from the dataset, then we allocate 2^q slots for all insertions by setting $q = \lceil \log_2(n) \rceil$. We next vary $r \in \{5, 6, 7, 8, 9, 10, 11\}$ and keep track of the seven possible sizes of the ADAPTIVEQF in each dataset.

For each dataset, we construct an ADA-BF [12] and Fast PLBF [44] by taking the corresponding size of the ADAPTIVEQF and subtracting the size of the trained model to obtain the space budget of the backup filters. For ADA-BF, we set $k_{min} = 8, k_{max} = 11, c_{min} = 2.1$, and $c_{max} = 2.6$, while for Fast PLBF we use $N = 1000$ and $k = 5$.

We also construct a stacked filter [14] matching the size of the ADAPTIVEQF. During construction, the stacked filter is given the first 25% of queries and their true results to learn the distribution of frequently occurring negatives.

This setup allows us to directly compare the FPR-space trade-off for each filter. Although each subsequent learned filter for a dataset has a smaller proportion of space dedicated to its internal model, we can now evaluate the effectiveness of the usage of the filters rather than having a confounding variable in the potentially improving accuracy of the model as its allowed space grows.

Adaptive filter reverse map. The adaptive filter requires a reverse map to recover original keys during adaptation. For an insertion set of size n , the reverse map is $O(n)$ in size and is therefore stored on disk and is accessed only upon false positives [50]. In production deployments, the backing database itself typically serves as the reverse map: since false positives already trigger disk accesses to verify membership, adaptation adds negligible overhead by reusing this lookup [50].

To isolate in-memory filter performance from disk I/O effects, all our experiments use in-memory implementations, including an in-memory chaining hash table for the reverse map. This ensures runtime measurements reflect actual filter operation costs rather than disk latency.

5.5 Training learned filters

Between trials, a new model is trained before constructing the filters, with all learned filters using the same model. We start by comparing the size and accuracy of `sklearn`'s `RandomForestClassifier`, `DecisionTreeClassifier`, and `LogisticRegression` models [39]. The logistic regression models are expected to be the smallest, followed by the decision trees, with random forests serving as the largest models.

The parameters were initially chosen by performing a grid search on a set of candidate parameter values which were expected to fit under the size of the smallest ADAPTIVEQF (guaranteeing space for backup filters), scoring based on the balanced accuracy across positive and negative values. Some grid search results still exceeded the size of the smallest ADAPTIVEQF, so those parameters were manually adjusted towards smaller values. Each dataset has different values for the model parameters, as described in [Table 2](#).

Dataset Name	Estimators (Forest)	Leaf Nodes (Forest)	Leaf Nodes (Tree)	C (Logistic)
URL	30	10	320	0.1
Ember	10	320	1,280	0.00001
Shalla	20	1,280	1,280	10
Caida	10	1,280	1,280	0.00001

Table 2: Summary of model parameters for datasets.

From a dataset, we randomly draw 30% of the negative keys and all of the positive keys as the training set, then use all of the negative keys and positive keys as the testing set. Example model sizes and accuracies from one trial of model training using the corresponding parameters from [Table 2](#) are included in [Table 3](#), which indicate that lower model sizes correspond to lower accuracy.

Dataset	Random Forest		Decision Tree		Logistic Regression	
	Size (KB)	Accuracy	Size (KB)	Accuracy	Size (KB)	Accuracy
URL	67	0.94	52	0.96	1	0.90
Ember	515	0.96	206	0.97	10	0.53
Shalla	4,102	0.7	206	0.71	1	0.63
Caida	2,052	0.97	206	0.97	1	0.51

Table 3: Example (rounded) model sizes and accuracies per dataset.

Since the *decision trees* exhibit competitive accuracy while taking moderately low space when compared to the other models ([Table 3](#)), the learned filters in the false positive rate experiments in [Section 6](#) use *decision tree* models. For construction and query time experiments, we still compare all model variants of the learned filters.

Vectorization. To employ the models, we adapted our feature vectorization methods to the dataset. To train the Malicious URL and Shalla models, 20 URL features such as hostname length, character counts, and number of directories were vectorized using an approach based on [40]. For the Ember model, we used the vectorized features defined by the benchmark [2]. For the CAIDA model, we vectorized the source and destination IP addresses and trained models to predict whether a network trace followed the TCP or UDP protocol.

Training set proportion. We run a short experiment increasing the proportion of negative keys included in the training set and record the resulting FPR of the learned filters on 10 million uniformly random queries on the original dataset. Across trials, the training set consists of all positive keys and a varying number of negative keys. For each of the three trials, we set the learned filter size to match an ADAPTIVEQF with $q = \lceil \log_2(n) \rceil$ and $r = 5$. [Figure 7](#) demonstrates that across trials, the median FPRs for all filters and models stayed relatively consistent with only a slight negative trend with the URL dataset, so we determine a train set proportion of 30% negative keys to be sufficient for later experiments.

When using the whole positive key set for training a model, the proportion of negative keys included in the training set can have low correlation with the quality of learned filter predictions on the overall dataset.

Model space proportion. Later experiments fix the parameters of the learned model while changing the size of the backup filter. We run a short experiment considering the opposite direction: how changing the model size affects performance when the overall filter size is fixed. We perform this experiment by fixing the learned filters to use large Random Forest Classifiers that gradually increase in size.

Across trials, we increase the number of leaf nodes used in the Random Forest Classifier. We fix the overall size of the learned filter to be larger than the model with the most leaf nodes and use the same size for each filter within the same dataset (described further in [Table 4](#)). Any remaining space in the total filter size after building the model is allocated to the backup filters. After inserting the positive keys into the filter, we record the resulting false positive rates after performing 10 million uniformly random queries on each dataset.

Dataset Name	Estimator Count	Min Leaf Nodes	Max Leaf Nodes	Filter Size (Bytes)
URL	30	5	30	500,000
Ember	80	2	10	70,000
Shalla	150	20	140	4,000,000
Caida	120	20	100	3,000,000

Table 4: Parameters used in model proportion experiments.

As anticipated from [Theorem 1](#), [Fig. 6](#) demonstrates that across all datasets, decreasing the proportion of space dedicated to backup filters eventually leads to an increase in false positive rate because the learned filter becomes overly dependent on model predictions. With less allotted space, the backup filters become more prone to reporting false positives due to an increased likelihood of hash collisions, reducing the benefits they provide for checking the model predictions.

Learned filters need sufficient space budget for backup filters to offset false positives generated by model predictions—if a larger, complex model is needed, then the overall false positive rate of the learned filter may increase.

5.6 Query Generation

To simulate alternative filter uses, we consider four possible types of distributions which the query workload Q follows.

One-pass. In the one-pass test, each element in the dataset is queried once. Notably, this test was used in the empirical analysis of Ada-BF [12] and Fast PLBF [44] in their respective papers.

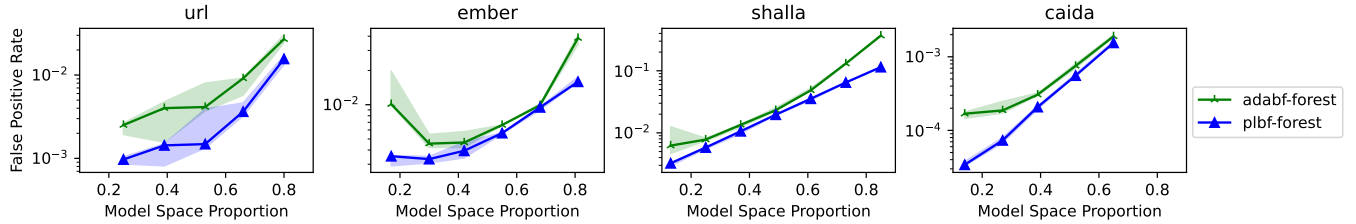


Figure 6: Effect of increasing proportion of (fixed) filter space dedicated to model on FPR (10M uniform queries on each dataset). Increasing the space usage of the model in a learned filter corresponds to an increased FPR.

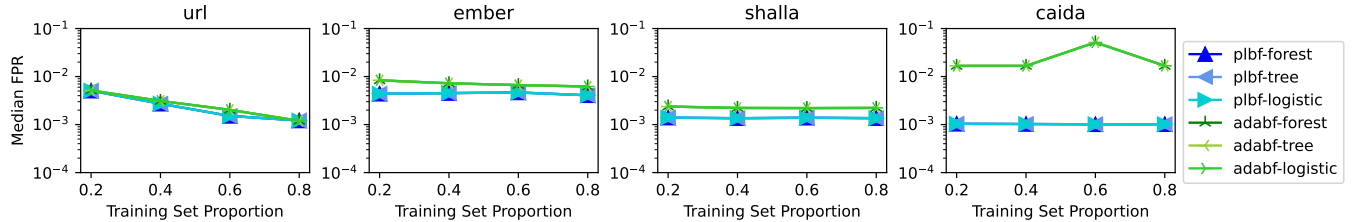


Figure 7: Effect of train set negative key proportion on median FPR (10M uniform queries on each dataset). Little correlation is shown between the proportion of negative keys used for training and the learned filter's performance.

Uniform. For this test, an element from the given dataset is chosen uniformly at random, for a total of 10 million queries.

Zipfian. To follow a Zipfian distribution, the probability of drawing an element x at index i of the dataset is proportional to $1/i^z$, where z is some constant. Distributions following this power-law are similar to real-world practical workloads where a few queries are very highly repeated [27, 51]. For this test, we set $z = 1.5$ and randomly draw queries from the given dataset 10 million times following this distribution.

Adversarial. We define an *adversarial query* as one drawn from a set of likely false positives. An "adversary" is given sufficient time to learn these candidate adversarial queries and aims to issue queries which increase the filter's overall FPR. In practice, adversaries can discover false positives through timing attacks, as positive and negative queries will have different latencies due to disk accesses.

For the adversarial query test, we perform tests in which the proportion of adversarial queries is $d \in \{0.02, 0.04, 0.06, 0.08, 0.10\}$. Our adversarial test is based on the workload presented by Wen et al. [50] to evaluate ADAPTIVEQF. Within a trial with d proportion of adversarial queries, we use $|Q| = 10M$ uniformly random queries from the dataset. In the first $|Q|/2$ queries, we record any false positives. For the remaining queries, every $(|Q|/2)/(d*|Q|)$ queries, we replace the next random query with a false positive, rotating through a list of false positives. We record the FPR after performing all queries, including adversarial ones.

During the adversarial test, for n filter insertions, we fix the ADAPTIVEQF to use $q = \lceil \log_2(n) \rceil$ and $r = 6$, then match that size when constructing the learned filters using parameters from Table 2.

5.7 Experiment categories

Varied query distributions. For this set of experiments, within a trial, we choose a dataset and construct a query set following one of the distributions (one-pass, uniform, Zipfian, adversarial), using the *same* query set for all filters within a dataset. Then, we construct the

filters according to Section 5.4 and insert all the positive keys into each filter.

We have all filters evaluate the complete query set and record the resulting FPR. We perform three trials, where in each trial we rebuild all filters (including retraining models), but the query set is not changed for the dataset. When performing the adversarial test, we chose not to use the adaptive variant of the stacked filter because it requires as input the distribution of the negative queries in the workload, which will change according to the false positives which the adversary detects.

Dynamic workload. For this experiment, we emulate the setting where the contents of the filter change in distribution while queries are performed. We first construct an ADAPTIVEQF, fixing it to use $q = \lceil \log_2(n) \rceil$ and $r = 5$ for datasets with n positive keys. We construct an ADA-BF and PLBF to each use the same space after training models according to the parameters described in Table 2. We also construct a stacked filter matching the space usage.

We start by defining a set of 10 million uniformly distributed queries from a dataset. Then, we begin querying the filters, reporting the instantaneous FPR whenever 1% of the queries have been finished. The *instantaneous false positive rate* is the FPR of a filter on all queries. The ADAPTIVEQF does not perform adaptations during this check.

Whenever 10% of queries are finished, we perform a churn of the dataset. We set aside a replacement set: a subset of the negative keys from the dataset equivalent in size to the set of positive keys. This size requirement ensures no negative keys are inserted as duplicates (we leave out the Shallal dataset since it has more positive than negative keys). There are 10 churnd total, each with replacement size $n/5$. On the j -th churn, we swap a portion of the inserted keys and replacement set, starting with the keys in position $start = n/5 * (j\%5)$ and ending at position $start + n/5$. Overall, each churn replaces 20% of the inserted key set with negative keys, so while performing queries the insertion set is gradually completely replaced with non-keys before being returned to the original insertion set.

In response to churns, we rebuild the filters so that they have the correct contents. The learned filters' internal models are retrained on the new positive set, which is a common response to distribution shifts [22]. On each churn, the reconstructed stacked filter is given the new distribution of the dataset.

Construction and query times. To evaluate the time it takes to perform different operations on each filter, we perform separate experiments where the construction of the learned filters is adjusted. The original learned filter code from [12, 44] trains models separately and computes all scores for the insertion and query sets before passing them to stored filters which are sized according to the space budget—this process streamlines query processing for FPR analyses. We partially rewrite the filters to store the learned model. Now, during a query, the filters first perform model inference on a vectorized key to obtain a score and decide how to query its backup filter(s). This simulates a realistic use case in which a learned filter must respond to a query on the fly.

During construction, for each dataset, for a dataset with n positive keys, we set $q = \lceil \log_2(n) \rceil$ for the ADAPTIVEQF, set $r = 5$, then match the resulting size when constructing the learned and stacked filters. We run 3 trials of 10 million uniformly distributed queries, recording the median construction and amortized query times for each filter.

6 Analysis

6.1 Varied query distributions

The results for each test provide interesting insights into how the guarantees of learned, stacked, and adaptive filters compare. In the FPR-space graphs we obtain (Fig. 8, Fig. 9, Fig. 10), we have the total filter size (including the trained model, if any) on the x-axis and the FPR on the y-axis. In general, more memory-efficient data structures will have lower curved lines. We plot the median FPRs across 3 trials, then shade between the minimum and maximum values within trials to indicate the variability of the results.

One-pass. In Fig. 8, for the learned filters, we find that the PLBF outperforms both the ADAPTIVEQF and stacked filter. PLBF also performs better than the ADA-BF, but this is expected and was previously demonstrated in a comparison between the two learned filters [44].

Since the one-pass query distribution is essentially a uniform distribution, the stacked filter is able to use its knowledge of the distribution and reduce its false positive rate through layers of filters. Thus, it performs better than the ADAPTIVEQF, though it is still outperformed by the PLBF.

With the ADAPTIVEQF, since each query is only performed once, it is unable to take advantage of multiple corrected false positives. So, in this workload, the ADAPTIVEQF behaves similarly to a traditional quotient filter, corresponding to its relatively higher FPRs compared to the other filter types.

Uniform. With uniformly distributed queries, we find in Fig. 9 that with the learned filters, the reported false positive rates remain very similar to the results from the one-pass test, since the uniform query distribution matches the training set distribution, allowing the model results to be generalizable.

The stacked filter performance also remains consistent with its one-pass results, since the distribution shape of the sampled negative values is similar to that of the uniformly-distributed query workload.

Regarding the ADAPTIVEQF, the gap between its performance and that of the other filters has become closer. This is likely due to the ADAPTIVEQF now being able to take advantage of its false positive adaptations, so if any false positive queries are repeated the ADAPTIVEQF later correctly classifies them. In a uniform workload with a larger number of queries than unique elements, a false positive is more likely to repeat, allowing the ADAPTIVEQF more opportunities to benefit from its prior adaptations. In particular, since the URL dataset has the lowest number of unique negative values, its uniform workload contains the highest number of repeated negative queries across the datasets, resulting in the ADAPTIVEQF performing the best on the dataset.

Zipfian. Results in Fig. 10 highlight the significance of filters' theoretical assumptions on the distribution of the insertion and query sets.

For all datasets with an Zipfian query load, the learned filters have significantly varied FPRs, with minimum and maximum FPRs for the same filter variant potentially being orders of magnitude apart. The learned filters have particularly poor results in the Shalla dataset, with a maximum FPR close to 50%, but also reach near-zero FPRs on the other datasets. There are two main reasons why the learned filter may exhibit such variance on these Zipfian query workloads.

Firstly, the model may be making inaccurate predictions after training. Between trials, the model and filter were reconstructed. During training, the model may fit to data points which appear infrequently in the workload at the cost of lower accuracy on frequently queried elements. If the model predicts a higher score for a negative key, then it the key is more likely to be returned as a false positive.

Secondly, the learned filters are inherently unable to adapt. If the model predicts a false positive, it repeats this mistake when the query is repeated. If the model predicts a negative but the backup filter returns a false positive, it cannot make changes to the backup filter to adapt to the result. So, in the case of the Zipfian workload, increasing the repetitions of a query can have drastic effects on the filter's overall FPR if both the model and backup filters repeat mistakes which cannot be corrected, contributing to inconsistent results across trials. In the other direction, if correct model decisions are frequently repeated, the learned filter can achieve extremely low FPRs, such as in the Caida dataset.

The stacked filter uses its knowledge of the workload distribution well. For a Zipfian workload, the query sample that the filter used for optimization likely contained the set of highly repeated negative queries, allowing the stacked filter to store those values and greatly decrease the odds of them becoming false positives. So, the stacked filter demonstrates performance competitive with the ADAPTIVEQF, even outperforming it on the Caida dataset.

The ADAPTIVEQF also has a consistently low FPR. In a Zipfian query workload, if a false positive occurs, it is likely to be highly repeated. Out of all static query distributions, the Zipfian workload provides the greatest opportunity for the ADAPTIVEQF to benefit from adaptations, as demonstrated by its greatly improved performance compared to the one-pass and uniform workloads.

Adversarial. For the adversarial test (Fig. 11), as the proportion of adversarial queries increases, the learned filters demonstrate increasing FPR. Again, since the learned filters cannot adapt, repeating previous false positives results in an increased overall FPR. Overall, since learned filter FPRs are highly dependent on the model

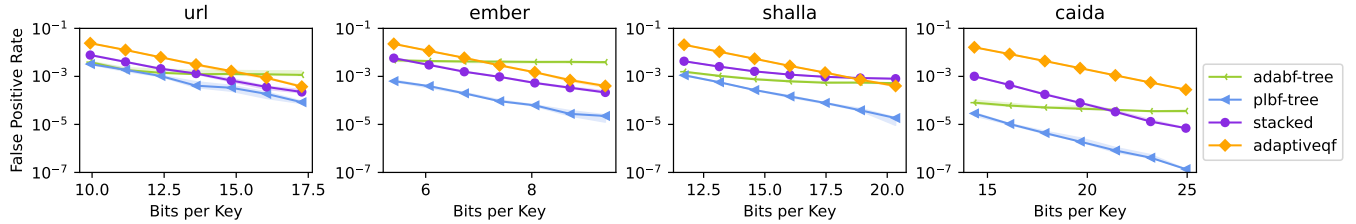
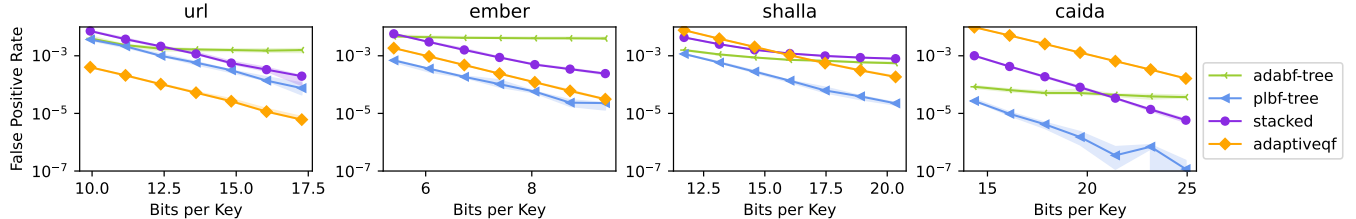
Figure 8: The FPR-space tradeoff for each dataset on a *one-pass* query test. Learned filters perform well, with stacked filters close behind.

Figure 9: The FPR-space tradeoff for each dataset on 10M uniformly distributed queries. Adaptive filters begin to catch up to stacked and learned filter performance.

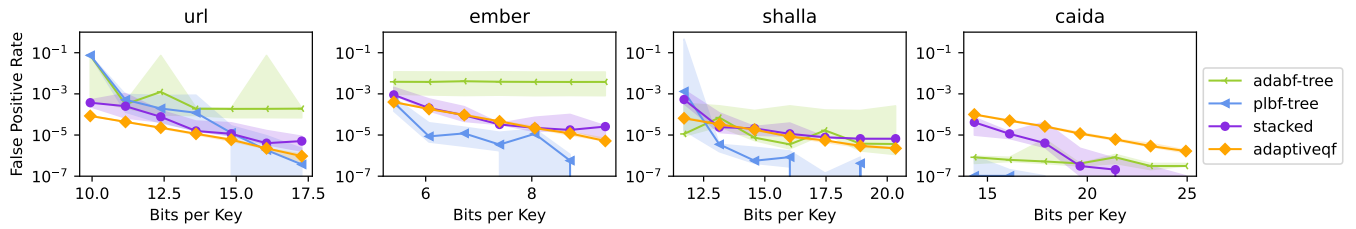
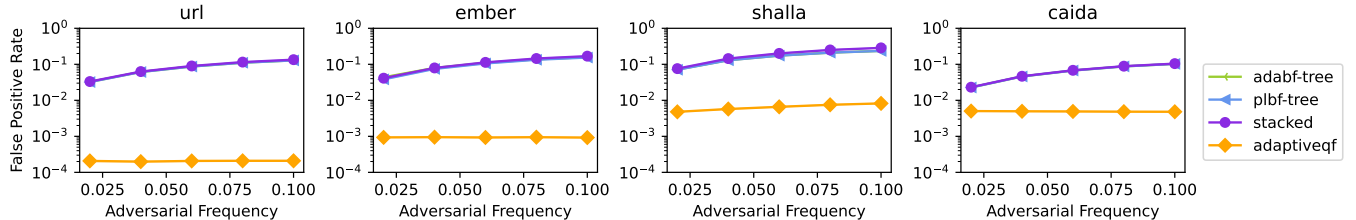
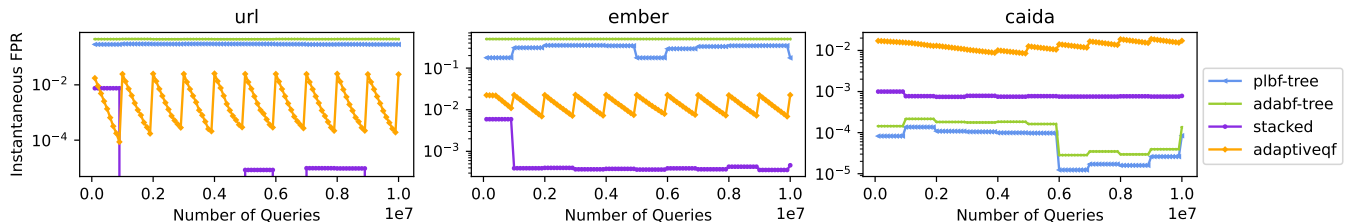


Figure 10: The FPR-space tradeoff for each dataset on 10M Zipfian distributed queries. Learned filter performance becomes variable, while stacked and adaptive filters exhibit consistent and low FPRs.

Figure 11: The effect of increasing the proportion of *adversarial* queries on the FPR of fixed-size filters for each dataset. Adaptive filters outperform all other filter types, whose results are identical and overlap.Figure 12: Instantaneous FPR of filters in response to *dynamic* workload with *model retraining*. Even with retraining, adaptive and stacked filters can still exhibit lower FPRs.

quality for a particular dataset, the benefits from utilizing learned predictions are inconsistent compared to the strong adaptability guarantees of adaptive filters. We confirm that, as described in [28],

learned filters are competitive when the query distribution is similar to the distribution that the filters are trained on.

The same drop in performance is present for the stacked filter: as the negative set changes, the stacked filter cannot update its contents,

resulting in increasing FPRs which are drastically higher compared to the ADAPTIVEQF. Likewise, stacked filters rely on the assumption that the query distribution remains relatively consistent, but introducing more negative queries makes the performance of the stacked filters less consistent.

For the ADAPTIVEQF, its FPR remains generally constant and low across all datasets with the adversarial workload. Adaptive filters are able to consistently alleviate errors caused by repeating a particular query in an arbitrary workload.

When query patterns include repeated (skewed) queries, adaptive filters often exhibit lower FPRs and more consistent negative correlations between space budget and FPR compared to learned and stacked filters. Learned filters are more appropriate for tasks where the query distribution closely matches the dataset distribution (such as one-pass classification), while stacked filters are appropriate when query workload distributions are not expected to change significantly.

6.2 Dynamic workload

Figure 12 indicates that retraining the model in response to dataset distribution shifts may improve FPR, but these effects are inconsistent. For instance, when the positive key set is replaced, the learned filters experience massive improvements in FPR on the Caida dataset, but on the URL and Ember datasets their FPR generally increased. With distribution shifts, the correlation between key features and presence in the set can weaken, making model predictions unreliable. However, even when models make good predictions, overall FPRs are still limited by the learned filters’ restriction to repeat the same predictions, resulting in static FPRs between churns. Additionally, Fig. 13 shows that the time needed to train a model is costly and can bottleneck the overall construction time of a filter, making this retraining procedure less practical.

For the stacked filters, their performance in Fig. 12 demonstrates that under conditions where periodic updates to the dataset are expected, simply relearning the distribution of negatives corresponds to highly competitive and consistent performance.

The robustness of the ADAPTIVEQF is demonstrated by Fig. 12. At every churn, the instantaneous FPR of spikes before rapidly decreasing due to adaptations, maintaining a relatively low overall FPR. The ADAPTIVEQF demonstrates that even with low FPRs, it can still adapt to achieve even lower FPRs over the course of a set of queries, while the learned filters remained fixed at particular FPRs between churns. However, in this workload, the ADAPTIVEQF does not adapt to enough false positives between churns to achieve instantaneous FPRs lower than the stacked filters.

Incorporating a machine learning model into a filter greatly limits its robustness. Models do not generalize well across dynamic workloads, and retraining does not guarantee improved performance on new distributions. The ability of a data structure to adapt to the query workload is crucial in these settings.

6.3 Construction and query times

Construction time. The construction times (in kiloseconds) for each filter and the proportion of time spent on different operations are plotted in Fig. 13. The construction operations were divided into

Filter Inserts (constructing the traditional filter structure and inserting elements into it), *Model Training* (constructing and training a machine learning model on a dataset), *Threshold Finding* (querying the model for scores and deciding how to use these scores to assign groups), and *Reverse Map Updates* (inserting elements into an auxiliary reverse map for the ADAPTIVEQF).

In all datasets, the construction of the ADA-BF is slowest largely due to the time it takes to find optimal score thresholds for group assignments. Note that future work could reduce this overhead—currently, the ADA-BF implementation [12] loops over and tests a range of thresholds. The FAST PLBF implementation [44] is an example of work which optimizes the construction of thresholds for prior learned filters [49].

In Fig. 13, we find that of the learned filter variants, those based on the PLBF are the fastest to construct. However, across all the datasets it is still $100\times$ slower to construct than the ADAPTIVEQF and stacked filter *at minimum*. This occurs because the construction time of the PLBF is dependent on its model training time. Even when score thresholds are efficiently established and backup filter construction is quick, model training time can take longer than the entire ADAPTIVEQF construction. This observation indicates that model training and construction is a significant overhead. Meanwhile, non-learned adaptive filters like the ADAPTIVEQF only consider the number of insertions (and potential adaptations for initial collisions) during construction time. The stacked filter takes some time to optimize based on the given negatives, but this process is still much faster than model training.

Learned filter construction time is highly dependent on the time it takes to train the model. In settings where more complex models are needed to capture correlations between features and classifications, it becomes less practical to rebuild learned filters in the face of new query distributions.

Query Time. The amortized query times (in milliseconds) and the proportion of time spent on different operations after performing experiments as described in Section 5.7 are plotted in Fig. 14. The included query operations were the *Filter Query* (probing the traditional filter(s) for an element), *Score Inference* (having an ML model generate a score for an element), and *Reverse Map Updates* (updating the ADAPTIVEQF using auxiliary data in response to false positives).

The most striking observation is that all amortized query times for both learned filters are up to $10^4\times$ slower than those of the ADAPTIVEQF and stacked filter. Across all datasets, learned filter query latency is dominated by the time spent performing model inference, even when the model is much smaller (in the cases of variants using decision trees or logistic regression models). This weakness contributes to learned filter query times *at least* $10^3\times$ slower than those of the ADAPTIVEQF. Notably, the vectorization of key features was implemented as a pre-processing step, and could serve as an additional overhead for on-the-fly query processing.

Meanwhile, the ADAPTIVEQF and stacked filter only depend on traditional filter operations and are extremely quick to process queries. However, due to stacked filters consisting of multiple layers of individual filters, the computational costs compound and result in query times up to $3\times$ slower than adaptive filters.

The computational cost of model inference in learned filters is orders of magnitude more expensive than traditional

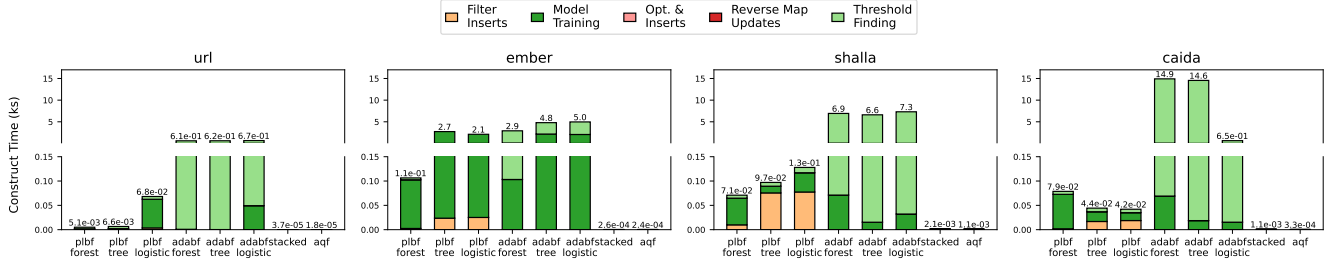


Figure 13: Overall filter *median construction time* on each dataset. Model training time dominates learned filter construction, resulting in stacked and adaptive filters demonstrating orders of magnitude faster construction.

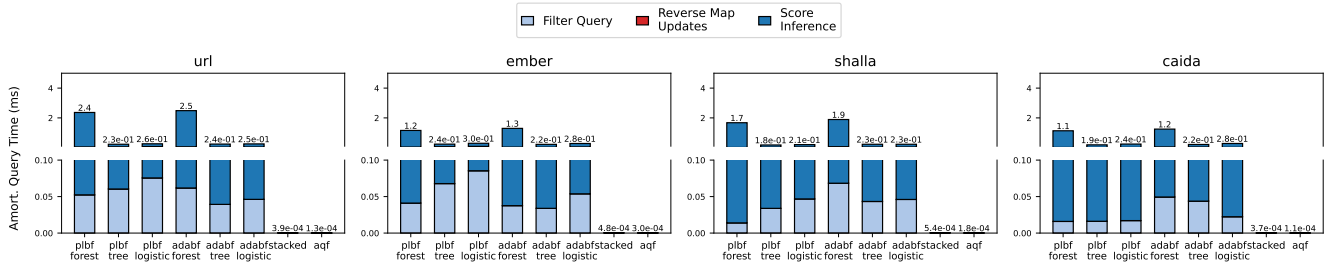


Figure 14: Overall filter *amortized query time* on each dataset. The cost of querying internal models for scores is much higher than that of querying backup filters, corresponding to stacked and adaptive filters exhibiting orders of magnitude faster queries.

filter operations even when simpler learned models are used, making learned filters impractical in settings where query throughput matters.

7 Discussion

Filters have been a cornerstone of systems design for over five decades, with recent paradigm-shifting advancements (learned, stacked, and adaptive filters) promising orders-of-magnitude improvements in FPRs. This paper provides the first unified evaluation, revealing that the choice of filter paradigm depends critically on application characteristics that prior work often overlooks. Our evaluation yields three principal insights:

(1) First, *learned filters are not a universal improvement over traditional filters*. While they achieve large reductions in false positive rate (up to $10^2 \times$ better) when query distributions match training data, this advantage can degrade under distribution shift, adversarial workloads, or repeated queries where ML model errors are amplified.

(2) Second, *computational overhead fundamentally changes the calculus*. Learned filters' model inference costs (up to $10^4 \times$ slower than traditional filter operations) have been systematically overlooked in prior evaluations. For applications where query throughput matters, this overhead can negate any space-efficiency gains. Adaptive and stacked filters, by contrast, maintain predictable and efficient query performance while still achieving competitive FPRs.

(3) Third, *robustness and generalizability vary across paradigms*. Adaptive filters provide the strongest and most robust guarantees: bounded false positive rates for arbitrary query sequences without requiring assumptions about workload distributions. Stacked filters offer excellent performance when query distributions are known and stable, achieving up to $10^3 \times$ lower false positive rates on skewed workloads. Learned filters, despite their sophistication,

tend to be least robust, exhibiting higher variance and potentially unpredictable behavior outside their training regime.

Future work: robust hybrids. Our study raises a critical question: can hybrid approaches combine the robustness of adaptive filters with the distribution-awareness of learned or stacked filters? Our evaluation framework and findings provide a foundation for exploring these directions by emphasizing considerations that should not be overlooked in filter evaluation and characterizing the performance of modern filter paradigms. We leave these potential designs for future work.

Acknowledgments

This work is supported by the NSF grants 2517201, 2513656, and DGE-2439018. We thank Yuvaraj Chesi and Aidan Ih for providing support for the implementation of the experiments.

References

[1] Ghada Almashaqbeh, Allison Bishop, and Hayder Tirmazi. 2025. Adversary Resilient Learned Bloom Filters. In *Advances in Cryptology (ASIACRYPT)*. Springer, 171–202. [doi:10.1007/978-95-5096-8_6](https://doi.org/10.1007/978-95-5096-8_6)

[2] H. S. Anderson and P. Roth. 2018. EMBER: An Open Dataset for Training Static PE Malware Machine Learning Models. *ArXiv e-prints* (April 2018). arXiv:1804.04637 [cs.CR]

[3] Michael A. Bender, Martin Farach-Colton, Mayank Goswami, Rob Johnson, Samuel McCauley, and Shikha Singh. 2018. Bloom Filters, Adaptivity, and the Dictionary Problem. In *FOCS*. 182–193. [doi:10.1109/FOCS.2018.00026](https://doi.org/10.1109/FOCS.2018.00026)

[4] Michael A. Bender, Martin Farach-Colton, Rob Johnson, Russell Kaner, Bradley C. Kuszmaul, Dzjelko Medjedovic, Pablo Montes, Pradeep Shetty, Richard P. Spillane, and Erez Zadok. 2012. Don’t Thrash: How to Cache Your Hash on Flash. *PVLDB* 5, 11 (2012), 1627 – 1637. [doi:10.14778/2350229.2350275](https://doi.org/10.14778/2350229.2350275)

[5] Burton H. Bloom. 1970. Space/time Trade-offs in Hash Coding With Allowable Errors. *Commun. ACM* 13, 7 (1970), 422–426. [doi:10.1145/362686.362692](https://doi.org/10.1145/362686.362692)

[6] Leo Breiman. 2001. Random Forests. In *Machine Learning*, Vol. 45. 5–32. [doi:10.1023/A:1010933404324](https://doi.org/10.1023/A:1010933404324)

[7] Alex D Breslow and Nuwan S Jayasena. 2018. Morton filters: faster, space-efficient cuckoo filters via biasing, compression, and decoupled logical sparsity. *PVLDB* 11, 9 (2018), 1041–1055. [doi:10.14778/3213880.3213884](https://doi.org/10.14778/3213880.3213884)

[8] Andrei Broder and Michael Mitzenmacher. 2004. Network applications of Bloom filters: A survey. *Internet Mathematics* 1, 4 (2004), 485–509. [doi:10.1080/15427951.2004.10129096](https://doi.org/10.1080/15427951.2004.10129096)

[9] Caida. 2016. Anonymized Internet Traces 2016. https://www.caida.org/catalog/datasets/passive_dataset/.

[10] Zhichao Cao, Siying Dong, Sagar Vemuri, and David HC Du. 2020. Characterizing, modeling, and benchmarking RocksDB key-value workloads at Facebook. In *18th USENIX Conference on File and Storage Technologies (FAST)*. 209–223. <https://www.usenix.org/conference/fast20/presentation/cao-zhichao>

[11] Alex Conway, Martin Farach-Colton, and Rob Johnson. 2023. SplinterDB and Maplets: Improving the Tradeoffs in Key-Value Store Compaction Policy. *PACMOD (SIGMOD)* 1, 1, Article 49 (2023), 27 pages. [doi:10.1145/3588726](https://doi.org/10.1145/3588726)

[12] Zhenwei Dai and Anshumali Shrivastava. 2020. Adaptive learned Bloom filter (ada-bf): Efficient utilization of the classifier with application to real-time information filtering on the web. *NeurIPS* 33 (2020), 11700–11710. <https://proceedings.neurips.cc/paper/2020/hash/86b94dae7c6517ec1ac767fd2c136580-Abstract.html>

[13] Niv Dayan, Ioana Bercea, Pedro Reviriego, and Rasmus Pagh. 2023. InfiniFilter: Expanding Filters to Infinity and Beyond. *PACMOD (SIGMOD)* 1, 2, Article 140 (2023), 27 pages. [doi:10.1145/3589285](https://doi.org/10.1145/3589285)

[14] Kyle Deeds, Brian Hentschel, and Stratos Idreos. 2020. Stacked filters: learning to filter by structure. *PVLDB* 14, 4 (2020), 600–612. [doi:10.14778/3436905.3436919](https://doi.org/10.14778/3436905.3436919)

[15] Cristian Diaconu, Craig Freedman, Erik Ismert, Per-Ake Larson, Pravin Mittal, Ryan Stonecipher, Nitin Verma, and Mike Zwilling. 2013. Hekaton: SQL server’s memory-optimized OLTP engine. In *SIGMOD*. 1243–1254. [doi:10.1145/2463676.2463710](https://doi.org/10.1145/2463676.2463710)

[16] Martin Dietzfelbinger, Peter C Dillinger, Lorenz Hübschle-Schneider, Peter Sanders, and Stefan Walzer. 2026. Ribbon: Fast Succinct Static Retrieval and Approximate Membership. *JACM* (2026). [doi:10.1145/3785417](https://doi.org/10.1145/3785417)

[17] Peter C. Dillinger and Panagiotis (Pete) Manolios. 2009. Fast, All-Purpose State Storage. In *Proceedings of the 16th International SPIN Workshop on Model Checking Software*. Springer, 12–31. [doi:10.1007/978-3-642-02652-2_6](https://doi.org/10.1007/978-3-642-02652-2_6)

[18] Gil Einizer and Roy Friedman. 2016. Counting with TinyTable: Every Bit Counts!. In *Proceedings of the 17th International Conference on Distributed Computing and Networking (ICDCN)*. ACM, Article 27, 10 pages. [doi:10.1145/283312.2833449](https://doi.org/10.1145/283312.2833449)

[19] Tomer Even, Guy Even, and Adam Morrison. 2022. Prefix Filter: Practically and Theoretically Better Than Bloom. *PVLDB* 15, 7 (2022), 1311–1323. [doi:10.14778/3523210.3523211](https://doi.org/10.14778/3523210.3523211)

[20] Bin Fan, Dave G Andersen, Michael Kaminsky, and Michael D Mitzenmacher. 2014. Cuckoo Filter: Practically Better Than Bloom. In *International Conference on emerging Networking Experiments and Technologies (CoNEXT)*. ACM, 75–88. [doi:10.1145/2674005.2674994](https://doi.org/10.1145/2674005.2674994)

[21] Matt Fredrikson, Somesh Jha, and Thomas Ristenpart. 2015. Model Inversion Attacks that Exploit Confidence Information and Basic Countermeasures. In *Proceedings of the 22nd ACM SIGSAC Conference on Computer and Communications Security (CCS)*. ACM, 1322–1333. [doi:10.1145/2810103.2813677](https://doi.org/10.1145/2810103.2813677)

[22] João Gama, Indr Zloboite, Albert Bifet, Mykola Pechenizkiy, and Abdelhamid Bouchachia. 2014. A survey on concept drift adaptation. *Comput. Surveys* 46, 4, Article 44 (2014), 37 pages. [doi:10.1145/2523813](https://doi.org/10.1145/2523813)

[23] Thomas Mueller Graf and Daniel Lemire. 2020. Xor Filters: Faster and Smaller Than Bloom and Cuckoo Filters. *Journal of Experimental Algorithms (JEA)* 25, 1 (2020), 1–16. [doi:10.1145/3376122](https://doi.org/10.1145/3376122)

[24] Shalla Secure Services KG. 2020. Shalla’s Blacklists. [Website discontinued. Snapshot available at <https://web.archive.org/web/20200501223254/http://www.shallalist.de/>. Last Accessed: May 2020.]

[25] Tim Kraska, Alex Beutel, Ed H. Chi, Jeffrey Dean, and Neoklis Polyzotis. 2018. The Case for Learned Index Structures. In *SIGMOD*. 489–504. [doi:10.1145/3183713.3196909](https://doi.org/10.1145/3183713.3196909)

[26] David J. Lee, Samuel McCauley, Shikha Singh, and Max Stein. 2021. Telescoping Filter: A Practical Adaptive Filter. In *29th Annual European Symposium on Algorithms (ESA) (LIPIcs, Vol. 204)*. 60:1–60:18. [doi:10.4230/LIPIcs.ESA.2021.60](https://doi.org/10.4230/LIPIcs.ESA.2021.60)

[27] Ryan Marcus. 2023. Learned Query Superoptimization. In *Workshop on Applied AI for Database Systems and Applications (AIDB’23)*. <https://ceur-ws.org/Vol-3462/AIDB5.pdf>

[28] Michael Mitzenmacher. 2018. A Model for Learned Bloom Filters and Optimizing by Sandwiching. In *NeurIPS*, Vol. 31. 462–471. <https://proceedings.neurips.cc/paper/2018/hash/049c89d1e729bb9930789c8ed59d48-Abstract.html>

[29] Michael Mitzenmacher, Salvatore Pontarelli, and Pedro Reviriego. 2020. Adaptive Cuckoo Filters. *ACM J. Exp. Algorithms* 25 (2020), 1–20. [doi:10.1145/3339504](https://doi.org/10.1145/3339504)

[30] Tianchi Mo, Michael A. Bender, Rathish Das, Martín Farach-Colton, and David Tench. 2026. Mitigating False Positives in Filters: to Adapt or to Cache? *TODS* (2026). [doi:10.1145/3786324](https://doi.org/10.1145/3786324)

[31] Israt Nisa, Prashant Pandey, Marquita Ellis, Leonid Oliker, Aydn Bulu, and Katherine Yelick. 2021. Distributed-memory k-mer counting on GPUs. In *2021 IEEE International Parallel and Distributed Processing Symposium (IPDPS)*. IEEE, 527–536. [doi:10.1109/IPDPS49936.2021.00061](https://doi.org/10.1109/IPDPS49936.2021.00061)

[32] Anna Pagh, Rasmus Pagh, and S Srinivasa Rao. 2005. An optimal Bloom filter replacement. In *Proceedings of the Sixteenth Annual ACM-SIAM Symposium on Discrete Algorithms (SODA)*. 823–829. <https://dl.acm.org/doi/10.5555/1070432.1070548>

[33] Prashant Pandey, Fatemeh Almودaresi, Michael A Bender, Michael Ferdman, Rob Johnson, and Rob Patro. 2018. Mantis: A fast, small, and exact large-scale sequence-search index. *Cell systems* 7, 2 (2018), 201–207. [doi:10.1016/j.cels.2018.05.021](https://doi.org/10.1016/j.cels.2018.05.021)

[34] Prashant Pandey, Michael A Bender, Rob Johnson, and Rob Patro. 2017. deBGR: an efficient and near-exact representation of the weighted de Bruijn graph. *Bioinformatics* 33, 14 (2017), i133–i141. [doi:10.1093/bioinformatics/btx261](https://doi.org/10.1093/bioinformatics/btx261)

[35] Prashant Pandey, Michael A Bender, Rob Johnson, and Rob Patro. 2017. A general-purpose counting filter: Making every bit count. In *SIGMOD*. 775–787. [doi:10.1145/3035918.3035963](https://doi.org/10.1145/3035918.3035963)

[36] Prashant Pandey, Michael A Bender, Rob Johnson, and Rob Patro. 2018. Squeakr: an exact and approximate k-mer counting system. *Bioinformatics* 34, 4 (2018), 568–575. [doi:10.1093/bioinformatics/btx636](https://doi.org/10.1093/bioinformatics/btx636)

[37] Prashant Pandey, Alex Conway, Joe Durie, Michael A. Bender, Martin Farach-Colton, and Rob Johnson. 2021. Vector Quotient Filters: Overcoming the Time/Space Trade-Off in Filter Design. In *SIGMOD*. ACM, 1386–1399. [doi:10.1145/3448016.3452841](https://doi.org/10.1145/3448016.3452841)

[38] Prashant Pandey, Shikha Singh, Michael A Bender, Jonathan W Berry, Martin Farach-Colton, Rob Johnson, Thomas M Kroeger, and Cynthia A Phillips. 2020. Timely reporting of heavy hitters using external memory. In *SIGMOD*. 1431–1446. [doi:10.1145/3318464.3380598](https://doi.org/10.1145/3318464.3380598)

[39] Fabian Pedregosa, Gael Varoquaux, Alexandre Gramfort, Vincent Michel, Bertrand Thirion, Olivier Grisel, Mathieu Blondel, Peter Prettenhofer, Ron Weiss, Vincent Dubourg, Jake VanderPlas, Alexandre Passos, David Cournapeau, Matthieu Brucher, Matthieu Perrot, and Edouard Duchesnay. 2011. Scikit-learn: Machine Learning in Python. *J. Mach. Learn. Res.* 12 (2011), 2825–2830. <https://jmlr.org/papers/v12/pedregosa11a.html>

[40] Aditya Pratama. 2024. Malicious URL Detection with ML (96.7% Acc). <https://www.kaggle.com/code/bytadit/malicious-url-detection-with-ml-96-7-acc/notebook>

[41] Joaquin Quiñero-Candela, Masashi Sugiyama, Anton Schwaighofer, and Neil D. Lawrence. 2009. *Dataset Shift in Machine Learning*. The MIT Press. [doi:10.7551/mitpress/978026217005.001.0001](https://doi.org/10.7551/mitpress/978026217005.001.0001)

[42] Pedro Reviriego, José Alberto Hernández, Zhenwei Dai, and Anshumali Shrivastava. 2021. Learned Bloom Filters in Adversarial Environments: A Malicious URL Detection Use-Case. In *2021 IEEE 22nd International Conference on High Performance Switching and Routing (HPSR)*. 1–6. [doi:10.1109/HPSR52026.2021.9481857](https://doi.org/10.1109/HPSR52026.2021.9481857)

[43] Kamil Salikhov, Gustavo Sacomoto, and Gregory Kucherov. 2014. Using cascading Bloom filters to improve the memory usage for de Bruijn graphs. *Algorithms for Molecular Biology* 9, 1 (2014), 2. [doi:10.1186/1748-7188-9-2](https://doi.org/10.1186/1748-7188-9-2)

[44] Atsuki Sato and Yusuke Matsui. 2023. Fast Partitioned Learned Bloom Filter. In *NeurIPS*, Vol. 36. https://proceedings.neurips.cc/paper_files/paper/2023/hash/7b2e844c52349134268e819a9b56b9e8-Abstract-Conference.html

[45] Franco Scarselli, Marco Gori, Ah Chung Tsoi, Markus Hagenbuchner, and Gabriele Monfardini. 2009. The Graph Neural Network Model. *IEEE Transactions on Neural Networks* 20, 1 (2009), 61–80. [doi:10.1109/TNN.2008.2005605](https://doi.org/10.1109/TNN.2008.2005605)

[46] Manu Siddhartha. 2021. Malicious URLs dataset. <https://www.kaggle.com/datasets/sid321axn/malicious-urls-dataset>

[47] Hayder Tirmazi. 2025. Adversarially Robust Bloom Filters: Privacy, Reductions, and Open Problems. arXiv:2501.15751 [cs.CR] <https://arxiv.org/abs/2501.15751>

[48] Cisco Umbrella. 2026. Umbrella Popularity List. <https://s3-us-west-1.amazonaws.com/umbrella-static/index.html> (Last accessed January 2026).

[49] Kapi Vaidya, Eric Knorr, Michael Mitzenmacher, and Tim Kraska. 2021. Partitioned Learned Bloom Filters. In *International Conference on Learning Representations (ICLR)*. <https://openreview.net/forum?id=6BRL0frMhW>

[50] Richard Wen, Hunter McCoy, David Tench, Guido Tagliavini, Michael Bender, Alex Conway, Martin Farach-Colton, Rob Johnson, and Prashant Pandey. 2024.

Adaptive Quotient Filters. *PACMOD (SIGMOD) 2, 4*, Article 192 (2024), 28 pages.
[doi:10.1145/3677128](https://doi.org/10.1145/3677128)

[51] Ziniu Wu, Ryan Marcus, Zhengchun Liu, Parimarjan Negi, Vikram Nathan, Pascal Pfeil, Gaurav Saxena, Mohammad Rahman, Balakrishnan Narayanaswamy, and

Tim Kraska. 2024. Stage: Query Execution Time Prediction in Amazon Redshift. In *Companion of the 2024 International Conference on Management of Data*. Association for Computing Machinery, 280–294. [doi:10.1145/3626246.3653391](https://doi.org/10.1145/3626246.3653391)

A Nomenclature

Symbol	Definition
FPR	(empirical) false positive rate
s	Model-output confidence score describing likelihood of key being present in set
t	Score threshold defining when learned filters query backup filters
b	Bits used per key in a learned filter's backup filter
α	The load factor of a filter
ζ	The number of bits used by a learned filter's internal ML model
f_m	False positive rate of a learned filter's ML model
f_n	False negative rate of a learned filter's ML model
f_b	FPR of a learned filter's backup filter(s)
k	Number of score-dependent groups keys are distributed across in a learned filter
c	How many times more non-keys each score-divided group of keys is expected to contain compared to the next group, used by the ADA-BF
N	Number of segments the score space is split into before assigning keys to groups, used by the PLBF
ϵ	Theoretical false positive rate for a filter
x	Example queried item
S	Set of keys represented by a filter
$h(x)$	Hash of element x
$h_0(x)$	Higher-order bits of $h(x)$ comprising the quotient
$h_1(x)$	Lower-order bits of $h(x)$ comprising the remainder
p	Length of fingerprint stored in ADAPTIVEQF
q	Length of hash quotient used by ADAPTIVEQF
r	Length of hash remainder and (future extensions) used by ADAPTIVEQF
n	Number of unique positive key elements inserted in a filter
i	Index of element in some permutation of its dataset
j	Current number of churns performed in the dynamic query workload
z	Zipfian constant describing power-law relation of randomly drawn elements
Q	Multiset of elements in the query workload
Q_N	Multiset of negative elements in the query workload
Q_{FP}	Multiset of false positives reported from query workload

B Filters

Filters, such as Bloom [5], quotient [4, 13, 17, 18, 35, 37], and cuckoo [7, 20] filters, maintain an approximate representation of a set. The approximate representation saves space by allowing queries to occasionally return a false positive. For a given false positive rate (FPR) ϵ , a membership query to a filter for set S is guaranteed to return present for any $x \in S$, while returning present with probability at least ϵ for any $x \notin S$. For $|S| = n$, space depends on (n, ϵ) and is typically far smaller than storing S explicitly.

B.1 Types of filters

Filters are commonly classified as *static*, *semi-dynamic*, or *dynamic*. Static filters (e.g., XOR [23], Ribbon [16] filters) require the complete item set before construction. Semi-dynamic filters like Bloom [5] and Prefix filters [19] support insertions but typically require an estimate of the final set size to meet a target FPR, which complicates deployments where $|S|$ is unknown. Dynamic filters (quotient [4, 13, 17, 18, 32, 35] and cuckoo [7, 20] filters) support both insertions and deletions and handle unknown sets and sizes, making them increasingly popular for real-world applications. Dynamic filters require $n \log(1/\epsilon) + \Omega(n)$ bits: quotient filters use $n \log(1/\epsilon) + 2.125n$ bits [35] and cuckoo filters use $n \log(1/\epsilon) + 3n$ bits [20]. Bloom filters use about $1.44 \cdot n \cdot \log(1/\epsilon)$ bits, but dynamic filters can approach $n \cdot \log(1/\epsilon) + \Omega(n)$ bits; Bloom filters are only smaller at very large ϵ (high FPR).

B.2 Fingerprint-based filters

State-of-the-art dynamic filters are fingerprint-based. They compactly store short, lossy fingerprints in a table using **quotienting** [32]. In quotienting, a p -bit fingerprint $h(x)$ is divided into two parts: the first q bits $h_0(x)$ is called the **quotient** and the remaining $r = p - q$ bits $h_1(x)$ is called the **remainder**. The quotient is stored implicitly and only the remainder is stored explicitly to save space.

Quotient filters [4, 17, 18, 35, 37] use Robin Hood hashing (a variant of linear probing) to store the remainders in a linear table. To resolve soft collisions (i.e., when two fingerprints share the same quotient but have different remainders) it uses 2-3 extra metadata bits to resolve collisions and efficiently perform queries.

C Modern filter paradigms

Recent advancements in filter design leverage dataset features, workload knowledge, or query feedback to improve false positive rates asymptotically. We provide short summaries of each of these new filter paradigms:

Learned Filter. During *initialization*, inserts keys into backup filter(s), then trains an internal ML model using features of those inserted keys. During *deployment*, the model generates a score describing the likelihood of a queried element being an inserted key, which is used to smartly decide how to query the structure's backup filters.

Stacked Filter. During *initialization*, a sample of the query workload is used to build layers of cascading filters, where the first large layer stores all positive keys, then the following layers alternate between storing all negative or all positive values which were false positives in the previous filter layer. During *deployment*, a queried element traverses the layers sequentially. If a layer returns negative, the element is returned as a (potentially false) positive if the layer stored negatives and returned as a (true) negative if the layer stored positives. If the element makes it through all layers of filters, the final filter determines the classification of the queried element.

Adaptive (Quotient) Filter. During *initialization*, in addition to storing all elements in a quotient filter, a (disk-resident) reverse map is maintained which associates each partial hash of an inserted element with the complete original key. During *deployment*, upon receiving feedback about a false positive result, the filter consults the reverse map to obtain sufficient information to update the structure and ensure the false positive is not repeated in the future.

D Learned filters

D.1 Base (sandwiched) learned filters

In the formal learned filter proposal [28], learned filters simply depended on a model score threshold to decide whether or not the the ML model’s prediction was a (potentially false) positive or a negative result which required verification from a backup filter. The sandwiched filter was proposed as an extension of this design, where an additional preliminary filter is checked before queries continue to the trained model. The preliminary filter ensures that (potentially many) true negatives cannot be misclassified by the ML model. The (sandwiched) learned filter structure is represented by Fig. 15. In their experimental evaluations, the ADA-BF, PLBF, and Stacked filters all demonstrated that their implementations provided better FPRs than the (sandwiched) learned filter [12, 14, 44]. Notably, it was found that in practical workloads, to optimize for space the sandwiched learned filter reduces to the base learned filter [12].

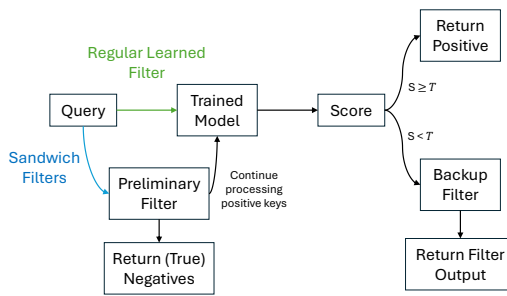


Figure 15: (Sandwiched) learned filter structure. A model prefilters positive keys before testing a backup filter for negative candidates. For the sandwich filter, an additional traditional filter is queried to remove true negatives before continuing to the trained model.

D.2 Learned filter distribution assumptions

Learned filters depend on the model training set closely matching the distribution of the query workload [28].

Theorem 2 formally describes this finding:

THEOREM 2. [28] For some learned Bloom filter, consider a test set T , and a query set Q , where T and Q are both sampled from some distribution. If x is the empirical false positive rate of the filter on T and y is its empirical false positive rate on Q , then

$$\Pr(|x - y| \geq \delta) \leq e^{-\Omega(\delta^2 \min(|T|, |Q|))}$$

Figures 10 to 12 describe experiments where the query workload distribution differs greatly from the training set distribution. In these cases, the learned filters demonstrated variable or worsened FPRs, affirming the insights from Theorem 2.

D.3 Model training results

Figures 16 to 18 demonstrate examples of the positive and negative key distributions across each dataset after one trial of model training using random forests, decision trees, and logistic regression models, respectively. The scores describe the model’s predicted likelihood that the given (vectorized) key is a positive key. Notably, when the model becomes extremely small in the case of the logistic regression

models (Table 3) in Fig. 18, the model predictions become unreliable, with positive and negative key scores demonstrating high overlap.

E Stacked Filters

Theorem 3 [14] formalizes the FPR and space guarantees of the stacked filter, stating that the overall false positive rate and space usage of the filter is dependent on the configuration of the filter layers comprising the overall structure.

THEOREM 3. [14] For a given stacked filter, let ψ represent the probability that a negative element from a query distribution is in the set of frequently queried negatives N_F , P represent the set of positive elements, l represent the number of layers in the structure, a_i represent the false positive rate of the i^{th} layer, and $s(\epsilon)$ represent the size in bits for a filter layer to achieve FPR ϵ .

Then the expected false positive rate of the stacked filter is

$$\psi \prod_{i=0}^{(l-1)/2} a_{2i+1} + (1-\psi) \left(\prod_{i=1}^l a_i + \sum_{i=1}^{(l-1)/2} \left(\prod_{j=1}^{2i-1} a_j \right) (1-a_{2i}) \right)$$

and the overall size of S is given by

$$\sum_{i=0}^{(l-1)/2} s(a_{2i+1}) * \left(\prod_{j=0}^{a_{2i}} \right) + \sum_{i=1}^{(l-1)/2} s(a_{2i}) * \frac{|N_F|}{|P|} * \left(\prod_{j=1}^i a_{2j-1} \right)$$

The initial layer storing all positives ends up dominating the space usage because the FPRs of each layer ensures that exponentially fewer elements must be stored in consecutive filter layers.

F Adaptive Filters

An example of how the ADAPTIVEQF uses quotienting for adaptations is depicted in Fig. 19. During an adaptation, when the remainder is extended it may take up additional quotient filter slots, so the ADAPTIVEQF additionally stores a few bits of metadata per element to keep track of which (larger) remainders correspond to which slot.

Additionally, we can describe the filter’s space and performance:

THEOREM 4. [50] For a set of size n and a target false positive probability ϵ , an ADAPTIVEQF will use $(1+o(1))n \log(1/\epsilon) + O(n)$ space. If the fraction of slots in use is α , then the cost of an insertion is $\Theta(\log n / (1-\alpha)^2)$ with high probability.

The size of the filter and the runtime operations are dependent on the size of the represented set, resulting in the quick filter operations represented in Figures 13 and 14.

G Gaps in modern filter evaluation

Existing research evaluates learned, adaptive, and stacked filters separately against traditional baselines but neglects direct comparisons between these modern approaches. Moreover, learned filter evaluations focus exclusively on stable workloads, ignoring adversarial vulnerabilities and performance under evolving distributions. Here, we identify key opportunities to improve filter evaluation.

G.1 Lack of comparative analysis

Current literature lacks extensive evaluation across modern filters: new learned filters compare their design with other learned filters and traditional (Bloom) filters, while adaptive filters compare their

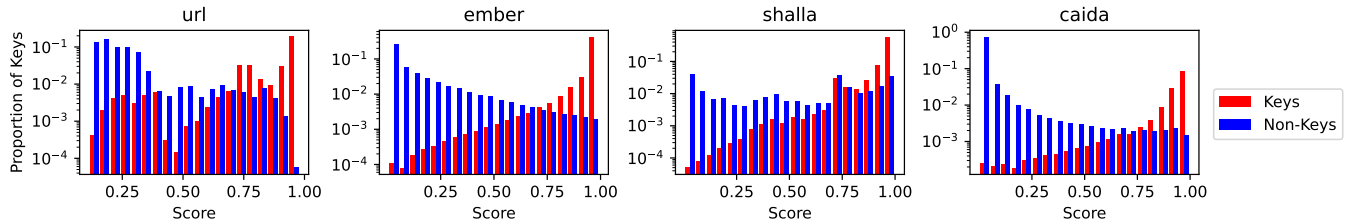


Figure 16: The distribution of *Random Forest* model scores for each dataset. Negative keys tend to skew towards lower scores, while positive keys skew towards higher scores.

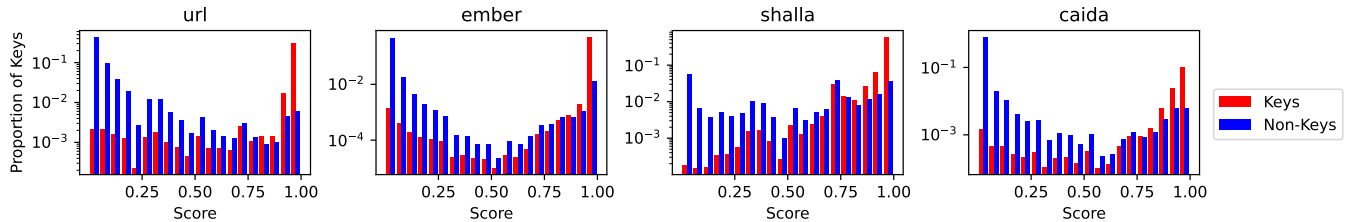


Figure 17: The distribution of *Decision Tree* model scores for each dataset. Positive keys still tend to skew towards higher scores, but negative keys have less consistent skew across datasets.

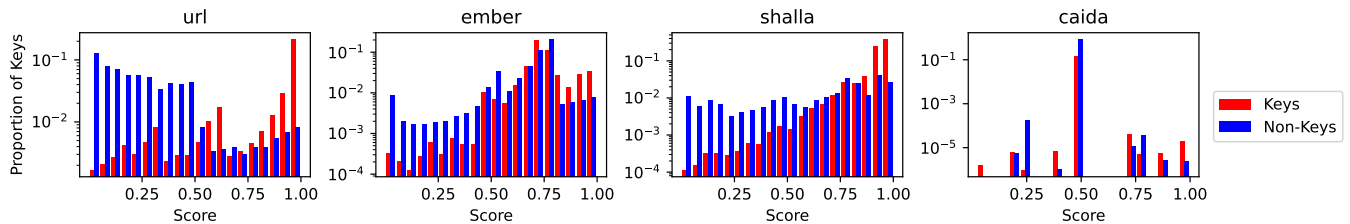


Figure 18: The distribution of *Logistic Regression* model scores for each dataset. Negative key scores have higher overlaps with positive key patterns.

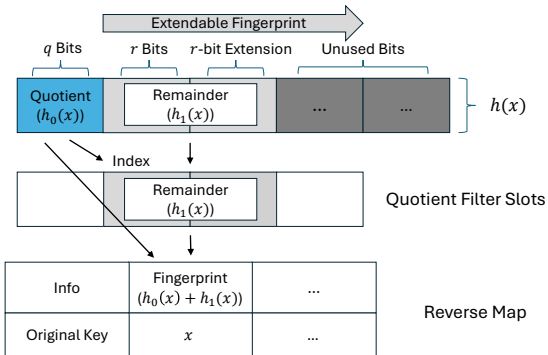


Figure 19: Example of key x being inserted into an *ADAPTIVEQF* and its entry into the on-disk reverse map. After finding the hash $h(x)$, the first q bits are used to determine where the fingerprint of the hash should be stored in the filter. The reverse map uses information about the fingerprint to find the original key, so that the original hash can be referenced for extensions in later adaptations.

proposed design with other adaptive filters and traditional filters. Existing literature on learned filters does not compare them against state of the art dynamic filters such as quotient and cuckoo filters and modern filters such as adaptive filters. Though, stacked filters

compare their performance with learned filters [14], there is no comprehensive comparison of all modern filter types together.

Without systematic comparative analysis of these modern filter types across multiple dimensions including space efficiency, query performance, construction time, and robustness guarantees, practitioners lack the guidance needed to select appropriate filtering strategies for their specific requirements.

G.2 Query distribution assumptions

Current evaluations of learned filters like ADA-BF and PLBF rely on the assumption that query distributions will closely match training distributions. This assumption underlies the theoretical guarantees provided by learned filters, as demonstrated by Mitzenmacher's [28] theorem showing that empirical false positive rates remain stable when test and query sets are drawn from the same distribution.

However, practical applications exhibit far more complex query patterns, including heavily skewed Zipfian distributions, dynamic workloads, and adversarial patterns where filter weaknesses are targeted. Existing learned filter evaluations do not reflect the hostile conditions present in security-critical applications such as malware detection, spam filtering, or intrusion detection systems.

This evaluation gap becomes particularly concerning when considering that learned filters inherit all the vulnerabilities of their underlying machine learning models, including susceptibility to

adversarial examples, model inversion attacks [21], and distribution shift exploits [41]. Traditional filters provide inherent resistance to adversarial queries because their behavior depends only on cryptographic hash functions rather than learned patterns that can be reverse-engineered or exploited, and for stronger security tests new secure designs for traditional filters have been proposed [47]. Recent work has demonstrated practical attacks on learned filters [42], but new designs focused on countering adaptive adversaries [1] make assumptions about the number of queries in the adversarial setting. The lack of adversarial evaluation in current literature means that the security implications of deploying learned filters in hostile environments remain largely unexplored, potentially creating significant vulnerabilities in production systems that rely on these approaches for security-critical filtering tasks.

G.3 Missing model cost analysis

Existing literature on learned filters exhibits a significant blind spot by focusing exclusively on space-accuracy trade-offs while ignoring the computational overhead introduced by model training/inference. These evaluations precompute the model score for each query and do *not* demonstrate the potential cost of model inference during filter queries. This simplification misrepresents the true performance characteristics of learned filters in practical deployments.

Comprehensive analysis reveals that model inference costs are much higher than traditional filter operations, with the exact overhead varying significantly based on model complexity, feature extraction requirements, and underlying hardware. For instance, Random Forest models [6] used in many learned filter implementations require traversing multiple decision trees and aggregating results, while neural network models [45] involve matrix multiplications and nonlinear activations. Additionally, the periodic retraining required to maintain model accuracy introduces substantial computational overheads that existing evaluations fail to consider, making the total cost of ownership significantly higher than traditional approaches.

While previous work did consider the query throughput of (sandwiched) learned filters [14], the evaluation will benefit by extending it to the current state of the art learned filters and adaptive filters.

G.4 Niche use cases and dataset selection

State-of-the-art learned filter designs are evaluated on specialized application datasets such as malware detection or malicious URL filtering [12, 44], where there are naturally strong correlations between observable features and set membership. These domains represent ideal conditions for learned approaches because the features used for classification (file characteristics, URL structure, network patterns) have been specifically chosen for their predictive power in distinguishing between positive and negative examples.

However, many practical filtering applications operate on data with weaker or nonexistent feature-membership correlations. For example, caching systems, database query optimization, and distributed systems coordination often need to filter arbitrary keys or identifiers that lack meaningful extractable features. The emphasis on specialized datasets in current literature makes it difficult to assess how learned filters would perform in general-purpose applications, potentially leading to overestimation of their broad applicability. Furthermore, the selection bias toward datasets with strong feature

correlations obscures the fundamental question of when learned approaches provide meaningful advantages over traditional methods.

G.5 Dynamic workload handling

Existing evaluations of learned filters typically assume static scenarios where both the underlying dataset and query patterns remain constant over time, failing to address the dynamic nature of real-world applications. This static evaluation methodology obscures critical questions about how learned filters degrade as workloads evolve and what maintenance strategies are required to sustain performance.

Real applications face continuously changing conditions including dataset growth, shifting query patterns, seasonal variations in access patterns, and evolving feature distributions that can rapidly obsolete trained models. The cost and complexity of retraining learned filters to maintain performance under these changing conditions represents a significant operational burden that current research largely ignores. Without understanding how frequently retraining is required, what triggers indicate degraded performance, and what graceful degradation strategies are available when retraining is delayed, it becomes impossible to assess the true total cost of ownership for learned filter deployments in dynamic environments.

G.6 Theoretical versus empirical guarantees

Traditional filters provide clear probabilistic guarantees that hold regardless of the specific data being filtered, enabling system designers to make precise capacity planning and performance predictions. In contrast, learned filters provide performance guarantees that depend on the quality of the underlying machine learning model, making it difficult to provide worst-case bounds essential for system design.

Mitzenmacher [28] provides theoretical analysis and proofs describing when a learned filter should have better space-accuracy trade-offs compared to traditional filters. The proposed theoretical model provides guidance on how to size the machine learning model and the backup filters given an overall space budget. However, current learned filter evaluations do not explicitly validate these claims in practice, lacking formal guidance on how to tune configuration parameters in practical systems; rather, they emphasize the overall performance of the filter according to some predetermined configuration. While their empirical results are promising, the theoretical guarantees of learned filters remain open for validation.

H Experiments and Analysis

H.1 Generating Zipfian queries

When generating Zipfian queries, we hash the indices of each element from a dataset before calculating the element’s likelihood of being drawn for the query workload. In sorted datasets, hashing the indices is crucial or else either only positive or only negative queries are more likely to be drawn. Figure 20 demonstrates how the Zipfian distribution on the Ember dataset appears, while Figure 21 shows an example of how hashing the indices influences the distribution for the Ember query workload that was used in practice.

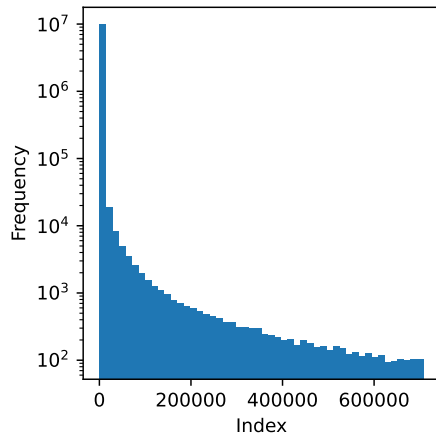


Figure 20: The query distribution for the Ember dataset prior to hashing. Following a power law, elements from the dataset are progressively less likely to be queried.

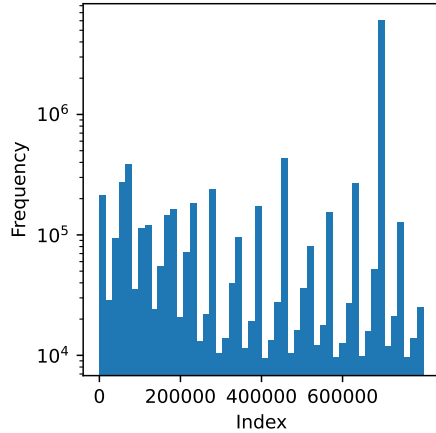


Figure 21: The query distribution for the Ember dataset after hashing. Some elements are still highly likely to be queried compared to others, but now the likelihood is independent of index (important since Ember is a sorted dataset).

H.2 Comparing model variants

Figures 22 to 25 describe how all filter variants compare on the FPR experiments, now including learned filters using random forest or logistic regression models.

Random forests. Table 3 describes that the random forest models used the largest space while still having similar accuracies to the decision trees used in the main FPR experiments. The new results indicate that the space usage of the random forest models make them unfit for learned filters. Since they now have less space dedicated to backup filters while still having similar model accuracy, learned filter variants using random forests generally have worse FPRs than decision trees.

Logistic regression. Table 3 describes that logistic regression models used the least space but demonstrated the worst classification accuracies. The new results indicate that this leads to inconsistent learned filter performance across different datasets. Generally, if

positive and negative key scores exhibit high overlap, learned filters are more likely to assign positive and negative keys to the same backup filter. Then, since the logistic regression models are small, learned filters leveraging these models have large space budgets for backup filters. On small datasets such as the URL dataset Table 1, a large space budget for a basic backup Bloom filter will result in near-zero FPRs, resulting in learned filter variants using logistic regression to have strong performance. However, on other datasets their performance falters, likely due to a combination of the backup Bloom filter's relatively low space-efficiency (compared to other traditional filter designs) and compounding model errors.

H.3 Dynamic experiment

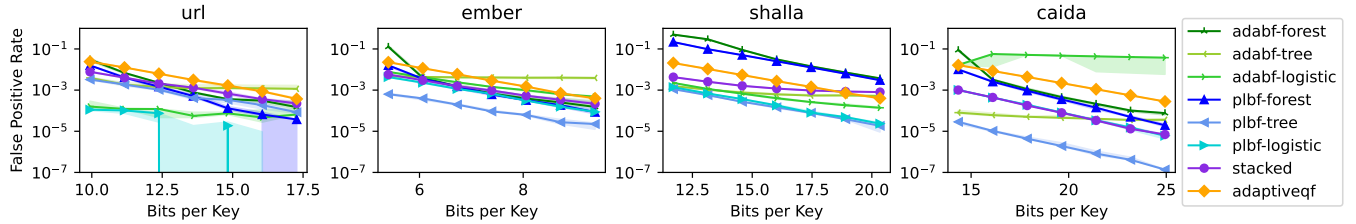
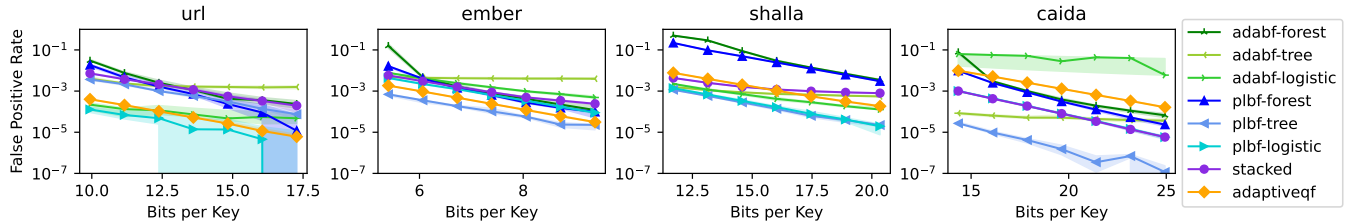
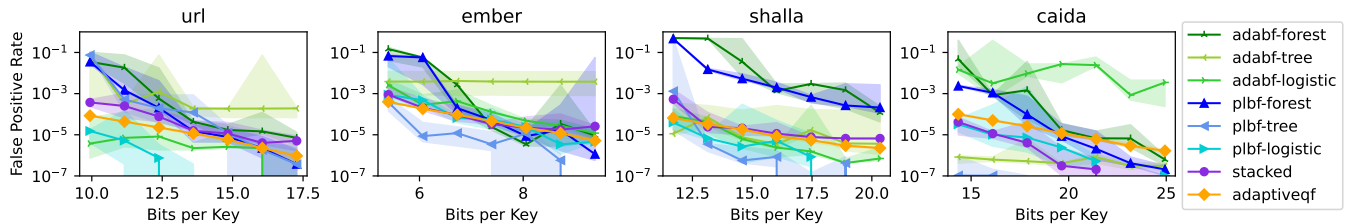
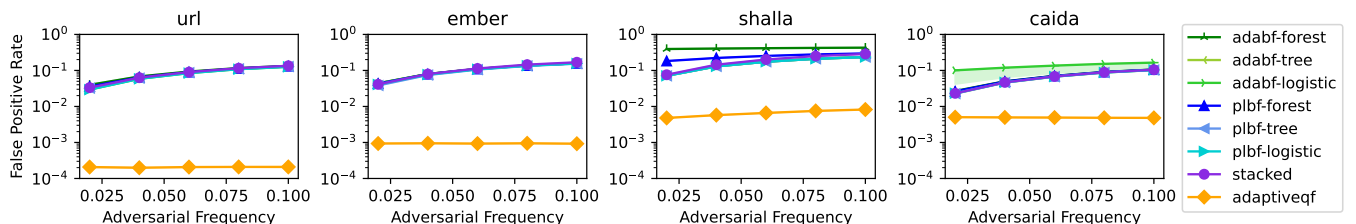
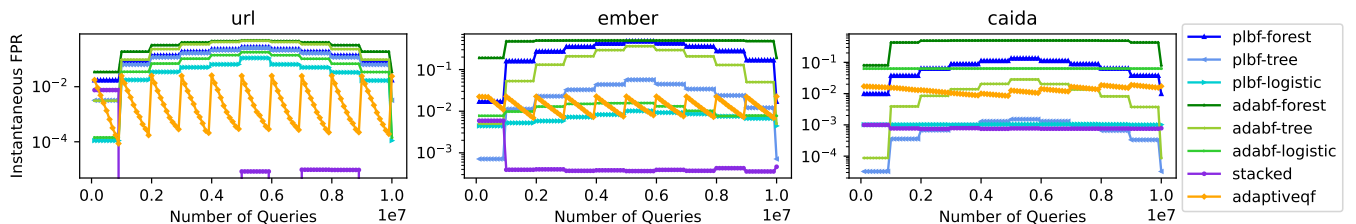
As a control of the dynamic experiment, we first perform a test where the learned filters do not retrain their models. We then repeat and allow the learned filters to retrain models during a churn, which is a common response to distribution shifts.

Figure 26 demonstrates that without retraining, both ADA-BF and PLBF have performance greatly depending on how well the set they were trained on matches the current insertion set. Between churns, their instantaneous FPRs are fixed, occasionally at very competitive values. However, as the dataset shifts, the model predictions across all variants become more inaccurate, and due to lack of adaptability the filters are stuck at high FPRs, sometimes even around $10^3 \times$ worse than the ADAPTIVEQF. They perform best only at the beginning and end of the dynamic test, when the datasets match the original set that the models were trained on.

On all model types, Fig. 27 still demonstrates that retraining models during periodic churns provides inconsistent effects on FPRs across different datasets.

H.4 Construction and query times

Note that for experiments involving query or construction times, key vectorization is considered as a separate step from filter operations, since some datasets already include features and do not require any vectorization. So, the time spent on this operation does *not* contribute to the learned filter results for these experiments, but in practice could serve as an additional overhead.

Figure 22: The FPR-space tradeoff for each dataset on a *one-pass* query test. Learned filters perform well, with stacked filters close behind.Figure 23: The FPR-space tradeoff for each dataset on 10M *uniformly* distributed queries. Adaptive filters begin to catch up to stacked and learned filter performance.Figure 24: The FPR-space tradeoff for each dataset on 10M *Zipfian* distributed queries. Learned filter performance becomes variable, while stacked and adaptive filters exhibit consistent and low FPRs.Figure 25: The effect of increasing the proportion of *adversarial* queries on the FPR of fixed-size filters for each dataset. Adaptive filters outperform all other filter types, whose results are identical and overlap.Figure 26: Instantaneous FPR of filters in response to *dynamic* workload (10M uniform queries on each dataset). Without retraining, learned filter FPRs degrade as the positive key set changes.

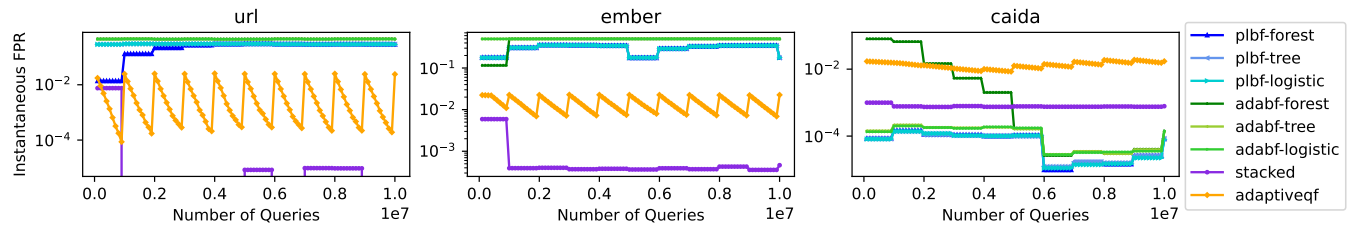


Figure 27: Instantaneous FPR of filters in response to *dynamic workload with model retraining*. Even with retraining, adaptive and stacked filters can still exhibit lower FPRs.